https://doi.org/10.5194/egusphere-2026-4106
Preprint. Discussion started: 14 July 2026

Combustion-Derived Organic Aerosols Enhance $PM_{2.5}$ Oxidative Potential in a Medium-Sized North China Plain City

Jing Cai[1,2], Yongchun Liu[3], Feixue Zheng[3], Dian Ding[4], Wei Du[5], Liang Yuan[6], Yingjie Zou[7], Lazong Suolang[8], Rongxiang Lu[8], Wanwei Li[8], Chao Liu[1,2], Xiaolong Fan[9,10], Qiaozhi Zha[4,11]*, Mengxiao Luan [8]*, Jiandong Wang[1,2]*

1. State Key Laboratory of Climate System Prediction and Risk Management, Nanjing University of Information Science and Technology, Nanjing, 210044, China
2. Collaborative Innovation Center on Forecast and Evaluation of Meteorological Disasters, School of Atmospheric Physics, Nanjing University of Information Science and Technology, Nanjing, 210044, China
3. Aerosol and Haze Laboratory, Beijing Advanced Innovation Center for Soft Matter Science and Engineering, Beijing University of Chemical Technology, Beijing, 100029, China
4. National Observation and Research Station for Atmospheric Processes and Environmental Change in Yangtze River Delta, Nanjing, 210023, China
5. Institute for Atmospheric and Earth System Research, Faculty of Science, University of Helsinki, Helsinki 00014, Finland
6. Chengdu Plain Urban Meteorology and Environment Observation and Research Station of Sichuan Province, School of Atmospheric Sciences, Chengdu University of Information Technology, Chengdu 610225, China
7. Shandong Weifang Provincial Eco-Environmental Monitoring Center, Weifang, 261053, China
8. School of Public Health, Shandong Second Medical University, Weifang 261053, China
9. State Key Laboratory of Advanced Environmental Technology, Institute of Urban Environment, Chinese Academy of Sciences, Xiamen 361021, China
10. Fujian Key Laboratory of Atmospheric Ozone Pollution Prevention, Institute of Urban Environment, Chinese Academy of Sciences, Xiamen 361021, China
11. Nanjing-Helsinki Institute in Atmospheric and Earth System Sciences, Nanjing University, Nanjing, China, 210023

Correspondence: Xiaolong Fan (xlfan@iue.ac.cn), Qiaozhi Zha (qiaozhi.zha@nju.edu.cn) and Mengxiao Luan (mxluan@sdsmu.edu.cn)

Abstract

Organic aerosol (OA) is a major component of $PM_{2.5}$ with significant health impacts, particularly in the highly populated NCP. However, characterizing OA composition, toxicity, and sources remains challenging. To address this, we conducted an intensive campaign throughout the 2023 – 2024 heating season in Weifang, a representative medium-sized NCP city. Despite overall air quality improvements, severe winter $PM_{2.5}$ pollution events still occurred, with a maximum concentration reaching 985 μg m^{-3}. Using a Chemical Ionization Time-of-Flight Mass Spectrometer equipped with a Filter Inlet for Gases and AEROsols (FIGAERO-CIMS), we obtained molecular composition and identified six clusters, linking them to sources resolved by positive matrix factorization (PMF) applied to the online dataset, including secondary

https://doi.org/10.5194/egusphere-2026-4106
Preprint. Discussion started: 14 July 2026

inorganics, biomass burning, vehicle emissions, coal combustion, and dust. To evaluate toxicity, we determined the oxidative potential (OP) in Weifang. While volume-normalized OP (OP_v) increased with both the degree of unsaturation and O:C ratios of OA, the compounds most positively correlated with mass-normalized OP (OP_m) exhibited an average carbon oxidation state of -0.5 and O:C of 0.5, indicating that moderately oxygenated OA possesses high OP activity. Multiple linear regression revealed that two combustion-derived groups drive OP: highly unsaturated $C_{10\text{-}15}$ compounds with ~10 oxygen atoms from solid fuel burning, and $C_{>15}$ compounds with <5 oxygen atoms or nitrogen-containing compounds from traffic emissions, which exhibited OP_m up to 23 times higher than the ambient average. Our study highlights the continued need for primary emission controls, particularly those targeting solid fuel combustion in the NCP region beyond its megacities.

https://doi.org/10.5194/egusphere-2026-4106
Preprint. Discussion started: 14 July 2026

1. Introduction

Organic aerosols (OA) typically account for 20% – 60% of ambient PM mass in the atmosphere and are the primary driver of aerosol cytotoxicity and adverse health outcomes, including respiratory inflammation, cardiovascular dysfunction, and premature mortality. In Chinese cities, OA constitutes 33% to 48% of fine particulate matter ($PM_{2.5}$) (Huang et al., 2014), and its relative contribution, particularly from secondary organic aerosol (SOA), has increased substantially in recent years (Chen et al., 2024).

Epidemiological studies have indicated strong associations between OA and adverse outcomes, including respiratory and cardiovascular hospital visits, morbidity, and mortality (Pye et al., 2021). Oxidative stress from certain pollutants, typically recognized as the pivotal mechanism underlying PM-related health hazards in toxicological studies, is quantified using oxidative potential (OP) as an indicator of redox activity. Some inhaled trace organic compounds were found to have high OP and corresponding high adverse health impacts. These compounds, such as quinones (e.g., 1,2-naphthoquinone, 1,4-phenanthraquinone), nitroaromatics, and humic-like substances (HULIS), stimulate excessive reactive oxygen species (ROS) generation, thereby disrupting antioxidant homeostasis and causing cellular damage and sustained inflammation (Fang et al., 2019; Chen et al., 2019; Shang et al., 2012). For example, the redox cycling of quinones and semiquinone radicals in the presence of ascorbic acid and iron can generate ROS, potentially increasing PM toxicity (Li et al., 2012). Similarly, HULIS may act as electron transfer intermediates to catalyze ROS production, and this process can be enhanced by reduced organic nitrogen compounds like alkaloids (Dou et al., 2015).

Due to the vast variations in the chemical composition, functional groups, redox properties, and interactions within OA across different sources, the resulting OP and health impacts are highly compound and source dependent (Bates et al., 2019). High-risk compounds that drive OP, such as nitro-/oxy-aromatics, polyphenols (Poly) and condensed aromatic amines, are more enriched in sources like residential combustion and biomass burning (Cao et al., 2025b; Zhang et al., 2025). Meanwhile, traffic-derived POA, enriched with PAHs and adipic acid (Zhang et al., 2016), also exhibits heightened OP and health risks. Furthermore, beyond primary emissions, the formation rate and toxicological potency of SOA are both highly dependent on the nature of its precursors and sources. For example, through rapid multi-generational

https://doi.org/10.5194/egusphere-2026-4106
Preprint. Discussion started: 14 July 2026

oxidation, anthropogenic aromatics like naphthalene and toluene produce organic compounds with much lower volatility (Wang et al., 2020a), a higher SOA production rate (Gu et al., 2023), and greater OP activity than biogenic precursors such as α-pinene (Tuet et al., 2017). Additionally, when fresh anthropogenic mixed with biogenic emissions, ROS generation and OP can be further enhanced due to quinone-terpenoid adduct stabilization of semiquinone radicals (Chen et al., 2026).

The North China Plain is a vast urban cluster with a population exceeding 340 million and a density of over 1,000 inhabitants per km², making it one of the world's most densely populated regions (Kulmala et al., 2021). In this region, significant amounts of carbonaceous aerosols and precursor VOCs are emitted from major sources such as solid fuel burning, vehicle exhaust, and agricultural activities. Based on the MEIC (Multi-resolution Emission Inventory model for Climate and air pollution research) inventory, in 2025, over 2.8×10^5 tons of organic carbon (OC) and 1.8×10^5 tons of black carbon (BC) were emitted in this region (Geng et al., 2024; Peng et al., 2019). However, while it is widely recognized that PM levels in this region exhibit spatial homogeneity validated by strong temporal correlations between cities within 250 km (Hu et al., 2014), the emission sources and intensity of carbonaceous aerosols display distinct spatiotemporal heterogeneity. Aerosol growth factors, OA composition, and formation pathways in smaller NCP cities (e.g., Xingtai and Handan) are distinct from those in Beijing due to different primary emissions and meteorological conditions (Wang et al., 2021; Gu et al., 2023). Gasoline and diesel vehicle emissions, for instance, are heavily concentrated in Beijing and Tianjin, where they constitute over 80% of transport-sector OC. In contrast, residential biofuel combustion is largely confined to Hebei and Shandong provinces, contributing 90% of the OC from this source with over 60% emitted during the heating season.

To the best of our knowledge, most previous studies on OA composition and its health impacts in the NCP have focused on megacities like Beijing and Tianjin. For example, Ma et al. (2018) identified biomass burning, coal combustion, waste incineration, vehicle emissions, and secondary formation as the dominant drivers of $PM_{2.5}$ OP in Beijing; Zheng et al. (2026) reported higher OP and carcinogenic risks during polluted events such as firework events and haze episodes; and Zhou et al. (2019) demonstrated that SOA dominates OP, contributing 60% of the total OP in Beijing. In contrast, the few studies conducted at rural NCP sites, mostly over short sampling periods, have

https://doi.org/10.5194/egusphere-2026-4106
Preprint. Discussion started: 14 July 2026

highlighted the significant contributions of nitrogen-containing organic compounds (Cao et al., 2026) and biomass burning to OP (Liu et al., 2024a).

The key toxic components and underlying health impact mechanisms of OA in broader NCP regions, especially in medium-sized cities, remain poorly constrained. This gap is particularly critical considering that over 80% (> 260 million) of the NCP population resides in over 50 medium-sized cities (1 – 10 million population). However, it remains unknown whether OP in those cities has declined as sharply as in Beijing recently, where strict regulations on residential burning have driven a drop in mass-normalized OP in the past decade (from 150 in 2015 to 24 pmol min^{-1} μg^{-1} in the 2020s (Zheng et al., 2026)). Bridging this gap by characterizing the key OA components that drive OP is vital for evaluating the health benefits of populations in these densely populated, medium-sized areas.

In this study, we conducted a field campaign covering the whole heating period from 2023 – 2024 in Weifang. We integrated offline filter sampling with molecular OA characterization via FIGAERO-CIMS (Cai et al., 2023)), alongside OP assays of ambient samples and standard chemicals, cluster analysis, and online $PM_{2.5}$ chemical speciation and PMF source apportionment. Our main objectives are: (1) to elucidate the near-molecular composition and concentrations of OA in Weifang; (2) to identify key OP-active organic compounds and their cluster characteristics, and to validate these findings using standard chemicals; and (3) to apportion the emission sources of high OP-active OA compounds in Weifang. This work provides new insights into the molecular-scale drivers of PM toxicity in medium-sized cities in the NCP region. Furthermore, these findings can inform targeted air quality management strategies based on particle composition and toxicological effects across the broader NCP, where the majority of the population resides in densely populated medium-sized cities.

2. Method

2.1 Measurement: Measurement site and filter collections

Field measurements in this study were conducted in Weifang; a city located in the NCP region and has a population over 9 million. The city is characterized by substantial primary emissions and vigorous secondary formation of pollutants. Consequently, its dense population faces heightened exposure to elevated concentrations of fine particulate matter.

https://doi.org/10.5194/egusphere-2026-4106
Preprint. Discussion started: 14 July 2026

Offline $PM_{2.5}$ Quartz filter samples collection in this study was conducted on the rooftop of Wenti Building in Shandong Second Medical University (36.7°N, 119.7°E), located in the urban area of Weifang city, using a Four-channel air particle sampler (TH-16A, Wuhan Tianhong Instrument Co., Ltd.) from Nov 15, 2023, to Mar 15, 2024, covering the whole heating season in Weifang. Offline samples (24-h) were collected from 12 am to 12 am every 3 days for FIGAERO-CIMS and dithiothreitol (DTT) tests. The sampling site has been introduced in a previous study (Li et al., 2025). All data have undergone strict quality control in accordance with the requirements of the corresponding instruments.

Online chemical components of $PM_{2.5}$ were measured in another near site covering the whole sampling period with a time resolution of 1 hour (see SI for a detailed description). Those components include black carbon (BC), measured by Aethalometer (AE33, Magee Scientific Inc., USA), total carbon (TC) measured by Total Carbon Analyzer (TCA-08, Magee Scientific Inc., USA), trace elements (including Al, K, Ca, Ti, Mn, Fe, Co, Cu, Zn, Se, and Pb) measured by an x-ray fluorescence instrument Online Atmospheric Heavy Metal Detector (AHMA-1000, NCS Testing Technology Co., Ltd., China) and water-soluble ions (sulfate, nitrate, ammonium, and chloride) were measured by a Monitor for AeRosols and Gases in ambient Air (MARGA, Metrohm Inc., Switzerland). Organic carbon (OC) was calculated as TC minus OC and OA was calculated as 1.4 times OC.

2.2 Analyze: FIGAERO-CIMS, DTT, Standard DTT analyze

Offline analysis of $PM_{2.5}$ filter samples was conducted utilizing a FIGAERO-CIMS (Aerodyne Research Inc., USA and Tofwerk AG, Switzerland) configured with I^- as the reagent ion (Zha et al., 2023; Lopez-Hilfiker et al., 2014). To generate the reagent ions, heated and dry ultra-high-purity N_2 was directed through a permeation tube containing liquid methyl iodide (CH_3I; Alfa Aesar, 99%) and subsequently into an X-ray source (Tofwerk AG, P-type), thereby producing I^- to charge the thermally desorbed compounds from the filter samples. For analysis, small circular punches (3.1×10^{-2} cm^2, 2 mm diameter) were taken from the collected filters. These punches were manually loaded into the FIGAERO-CIMS filter holder between two pre-baked, full-sized (25 mm diameter) Zefluor® Teflon filters, a method adapted from previous studies (Cai et al., 2023; Cai et al., 2022). The thermal desorption procedure with a uniform temperature ramping from 25 °C to

https://doi.org/10.5194/egusphere-2026-4106
Preprint. Discussion started: 14 July 2026

200 °C was deployed to analyze the OA. And the calibrations were conducted with levoglucosan ($C_6H_{10}O_5$) and succinic acid ($C_4H_6O_4$). The data was analyzed with Tof-ware (ver. 3.3.2) and 1,630 compounds were identified in the ambient samples. The OA compounds identified with FIGAERO-CIMS can be regarded as oxygenated since I^- is more favored to charge moderately oxygenated OA. Double Bond Equivalent (DBE), O to C ratio (O:C) and oxidation state (OS) of compounds were also calculated (see SI for a detailed description).

In our study, OA compounds identified by FIGAERO-CIMS were defined as CHOX ($C_{\geq 1}$, $H_{\geq 1}$, $O_{\geq 2}$, where X represents $N_{0\text{-}n}$, $S_{0\text{-}n}$, or both). These CHOX species were considered as oxygenated species since I^- ionization tends to select toward moderately oxygenated OA. Concentrations of CHOX were carefully calibrated using levoglucosan ($C_6H_{10}O_5$) and succinic acid ($C_4H_6O_4$). Specifically, integrated signals for lower molecular weight compounds (m/z < 120) were calibrated with succinic acid, while other compounds (m/z from 120 to 500) were calibrated with levoglucosan, as its sensitivity approaches the collision-limit of the FIGAERO-CIMS (Lopez-Hilfiker et al., 2016). Using this semi-quantitative method, we determined that the identified CHOX species constituted approximately 40 % of the total OA mass concentration during the study period.

The OP of ambient $PM_{2.5}$ samples and commercial standards was measured using the DTT assay. This well-established method has been described in detail previously (Ma et al., 2018; Cho et al., 2005) and is thus only briefly introduced here. Half of each collected ambient sample was ultrasonically extracted in 5.0 mL of purified water for 60 min in a water bath at 37 °C. The extracts were filtered through a 0.45 μm PTFE membrane filter. The dissolved samples in filtrates were then reacted with excess DTT and the consumption rate was measured by an ultraviolet-visible (UV-Vis) spectrophotometer (Ma et al., 2018; Cho et al., 2005). Therefore, it should be noted that water-insoluble components, including elemental carbon (EC), water-insoluble organics (e.g., HULIS), and insoluble metals, were not analyzed in the DTT analyses in this study. In total, 45 samples, 2 blanks were analyzed for this study, accompanied by daily standard calibration curves obtained before and after experiments (see Supporting Information for detailed methods). The volume normalized (OP_v) and mass normalized OP (OP_m) were calculated as Eq.1 to 3.

https://doi.org/10.5194/egusphere-2026-4106
Preprint. Discussion started: 14 July 2026

$$OP_{v\text{-}PM} = \frac{(Abs_b - Abs_a) \times DTTc}{RT \times V_{ambient}} \quad \text{Eq. 1}$$

$$OP_{m\text{-}PM} = \frac{(Abs_b - Abs_a) \times DTTc}{RT \times M_{ambient}} \quad \text{Eq. 2}$$

$$OP_{m\text{-}chem} = \frac{(Abs_b - Abs_a) \times DTTc}{RT \times M_{Chem}} \quad \text{Eq. 3}$$

Abs_a and Abs_b are the light absorption for each sample at time 0 and time b, respectively. $DTTc$ refers to DTT concentration (nmol), and RT is the reaction time at 37 °C. $V_{ambient}$, $M_{ambient}$ and M_{Chem} represent the volume of the ambient sample, the mass concentration of the ambient sample, and the added mass of the standard, respectively. Notably, our subsequent analysis validates the use of water extraction by identifying water-soluble OA (dominated by oxygenated species) as the primary driver of the measured OP, demonstrating significantly stronger correlations than transition metals (Fig. S6).

2.3 Data analyses

Hierarchical Cluster Analysis (HCA) clustering method is applied to classify OA offline samples based on their molecular-level composition and temporal variations. The analysis was conducted using R software (ver. 4.4.1) with 274 high concentration compounds with signal intensity > 0.05% of total CHOX and at least twice the background level which defined as the standard deviation of field blanks. The details for clustering methods have been given in SI.

The positive matrix factorization (PMF) model was utilized with online data with the resolution of 1-h for source apportionment of $PM_{2.5}$. The online $PM_{2.5}$ component data was imported into the Source Finder toolkit (SoFi, ver. 6.8.4), which communicates with the multi-linear engine (ME-2). The PMF model was conducted with a factor number from 2 to 7 and the results of 5 factors were chosen (see SI for a detailed description).

We applied both online source apportionment using PMF with $PM_{2.5}$ component data, and offline sample analyses utilizing FIGAERO-CIMS data with an HCA clustering model to characterize the source of OA. Although the two methods operate on different time scales and utilize distinct tracers, the strong temporal correlation between their results (r = 0.7 to 0.8 for most factors) indicates that the source apportionments from PMF and HCA are highly comparable. Furthermore, the consistency of inorganic and organic tracers across both models further solidifies these findings. A detailed comparison of

https://doi.org/10.5194/egusphere-2026-4106
Preprint. Discussion started: 14 July 2026

the organic clustering, organic tracers, and inorganic PMF results is presented in SI and Section 3.3.

3. Results

3.1 High levels of PM and OA in Weifang

Weifang displayed elevated gaseous pollutant concentrations compared to NCP megacities such as Beijing and Tianjin, where residential coal and biomass burning are restricted. During the same observation period (Nov 2023 to Mar 2024), Weifang's SO_2 (5 ppb) and NO_2 (17 ppb) levels were approximately twofold higher than those in Beijing (1.4 and 9.7 ppb, respectively) and Tianjin (2.5 and 10 ppb), revealing the ongoing significance of primary emissions. Furthermore, despite being only 300 – 400 km from Weifang, Beijing and Tianjin, a distance easily spanned by accumulation-mode PM transport, the NCP cannot be treated as a spatially homogenous emission region. This spatial heterogeneity directly affects the chemical composition and toxicity of regional air pollution, a conclusion further corroborated by the extreme PM levels during the episodes and Weifang's distinct OA composition.

Severe $PM_{2.5}$ pollution events were frequently observed in Weifang during the measurement period, with a mean $PM_{2.5}$ of 58 μg m^{-3} (Fig. 1a), and seven identified pollution episodes during which hourly levels exceeded 200 μg m^{-3}. The $PM_{2.5}$ concentration exhibited periodic cycles every 5 to 7 days, similar to those observed in Beijing which is typically driven by pollutant accumulation and cold front arrivals (Jia et al., 2008), However, a distinct daily cycle also emerged in Weifang, especially after January 2024, which peaked in the morning with gaseous pollutants (Fig. S2), underscoring the emissions influences (Fig. 3). The highest peak concentration (985 μg m^{-3}) occurred on Chinese New Year's Eve, coinciding with intense firework emissions (Feb 9 – 11, 2024). These findings indicate that, despite the general decline of $PM_{2.5}$ levels in megacities like Beijing (Chen et al., 2024; Dai et al., 2023; Chen et al., 2025a), autumn and wintertime air pollution may remain substantial across the broader NCP region. Specifically, nitrate was the most abundant species in $PM_{2.5}$ (16.6 μg m^{-3}, 29 %), followed by OA (12.3 μg m^{-3}, 22 %) and sulfate (7.6 μg m^{-3}, 13%). However, in Weifang, the correlation coefficient between $PM_{2.5}$ and OA (r = 0.80) was stronger than that with nitrate (r = 0.71), underscoring that OA emissions are the key driver to fine PM pollution, especially during extreme episodes.

https://doi.org/10.5194/egusphere-2026-4106
Preprint. Discussion started: 14 July 2026

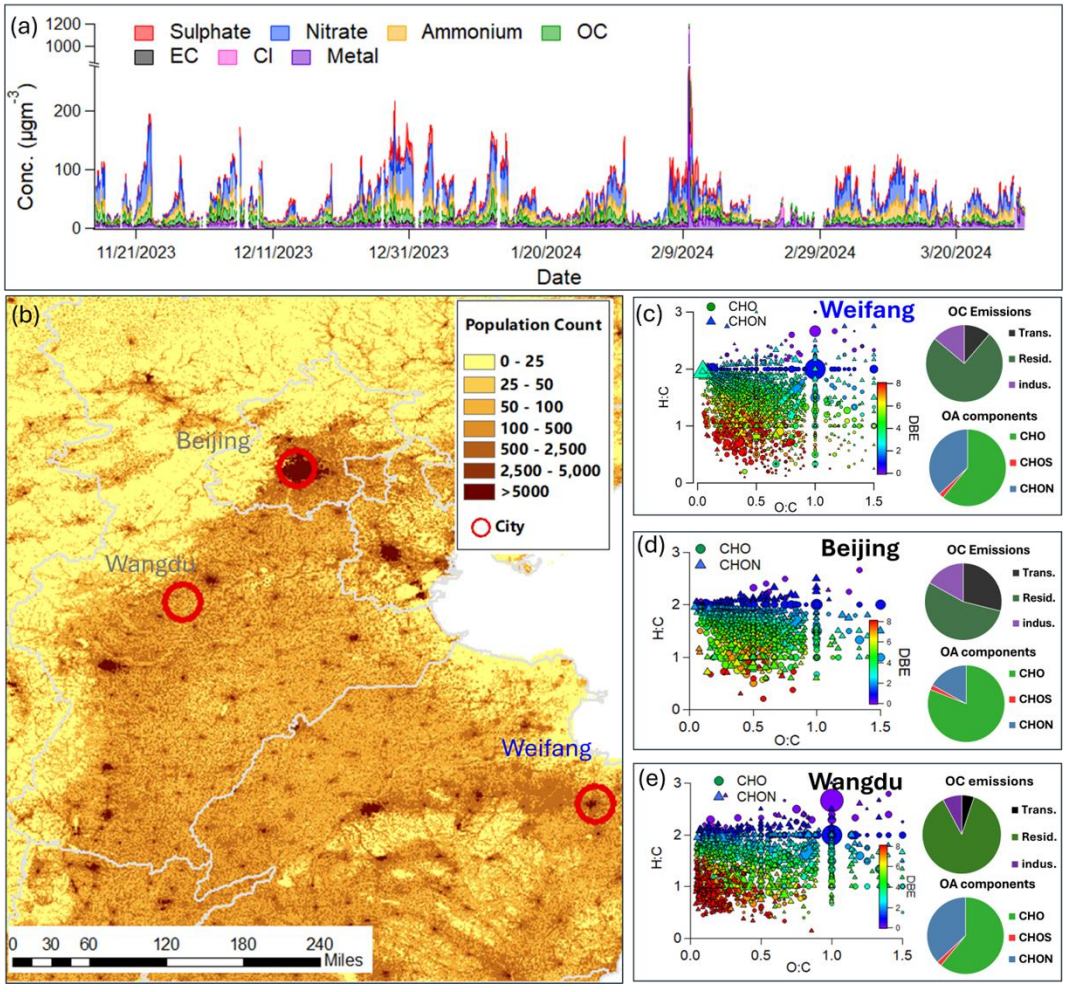

Figure 1. (a) Temporal variations of $PM_{2.5}$ and major chemical components during the sampling period; (b) Population density distribution in the North China Plain (data source: https://landscan.ornl.gov/); (c), (d), and (e) Van Krevelen (VK) diagrams for CHO and CHON compounds and group fractions (pie chart, green for CHO, blue for CHON and red for CHOS) from Beijing (BJ), Wangdu (WD), and Weifang (WF, this study) in autumn. The size area of dots was proportional to the fourth square root of corresponding integrated signals. Beijing and Wangdu data are adapted from Cai et al., 2022 (Cai et al., 2022) and Ren et al., 2022 (Ren et al., 2022), respectively. OC emission sections of each city were from MEIC (http://meicmodel.org.cn, (Geng et al., 2024)).

Based on FIGAERO-CIMS measurements, the observed OA in Weifang was classified into CHO, CHON, and CHOS groups to investigate its composition. These results were then compared with our previous heating-season measurements conducted in Beijing (Nov 2018, megacity site, population density > 5000 km^{-2}) and Wangdu (Jan, 2019, rural site, population density 500 – 2000 km^{-2}) in the NCP (Fig. 1b). In Weifang, CHO, CHON, and

https://doi.org/10.5194/egusphere-2026-4106
Preprint. Discussion started: 14 July 2026

CHOS accounted for 61%, 37%, and 2% of the OA signals, respectively (Fig. 1c). This compositional distribution closely similar to that of Wangdu (CHO: 67%, CHON: 30%, CHOS: 3%; (Ren et al., 2022)), but differed significantly from Beijing (CHO: 81%, CHON: 17%, CHOS: 2%; (Cai et al., 2022)). Notably, the CHON proportion in Weifang was comparable to Wangdu, a site heavily influenced by biomass burning during the harvesting and heating seasons. The elevated CHON fractions in Weifang and Wangdu are consistent with their higher NO_2 levels (36 ppb and 34 ppb on average, respectively, versus 29 ppb in Beijing) in autumn and winter, which are likely driven by local NOx concentrations and intense combustion activities (e.g., biomass and residential burning).

It is consistent with the emission inventories (MEIC) which suggest residential burning is the dominant OC source in Weifang, which is lower than Wangdu (87%) but substantially higher than in Beijing (54%). Consistent with this, a large fraction of levoglucosan (0.9 % in signal intensity) and compounds with DBE>4 comprised ~40% of the total OA by number during the measurement period (Fig. 1c), exceeding previously reported fractions in Beijing (20%) but close to those in Wangdu (40%). This indicates that as a medium-sized city in the NCP, Weifang is more heavily influenced by primary residential combustion emissions than megacities like Beijing, yet comparable to the rural Wangdu site, characterized by intense agricultural activities, as further validated by the high urea signal (Fig. 1e).

3.2 Sources of $PM_{2.5}$ in Weifang City

Hourly online water-soluble ions, OC/EC, and trace elements data were utilized to resolve major $PM_{2.5}$ sources in Weifang using the PMF method. Based on the source apportionment results, we further compared the contribution of different $PM_{2.5}$ sources and indicate the source origins of OA (Fig. 2a). The five-factor result was selected since adding more factors could not further improve the explanation of the residuals (Fig. S1). The identified sources include secondary inorganics (33%), biomass burning (26%), vehicle emissions (18%), coal combustion (13%) and dust (10%). Solid fuel burning (sum of biomass burning and coal combustion) contributed around 40% of total $PM_{2.5}$, implying the importance of residential emissions. The source apportionment results are further validated by their source profiles (Fig. S3), and their high correlation with organic and inorganic tracers. Detailed

https://doi.org/10.5194/egusphere-2026-4106
Preprint. Discussion started: 14 July 2026

information of source apportionment method and validation can be found in SI and the following section.

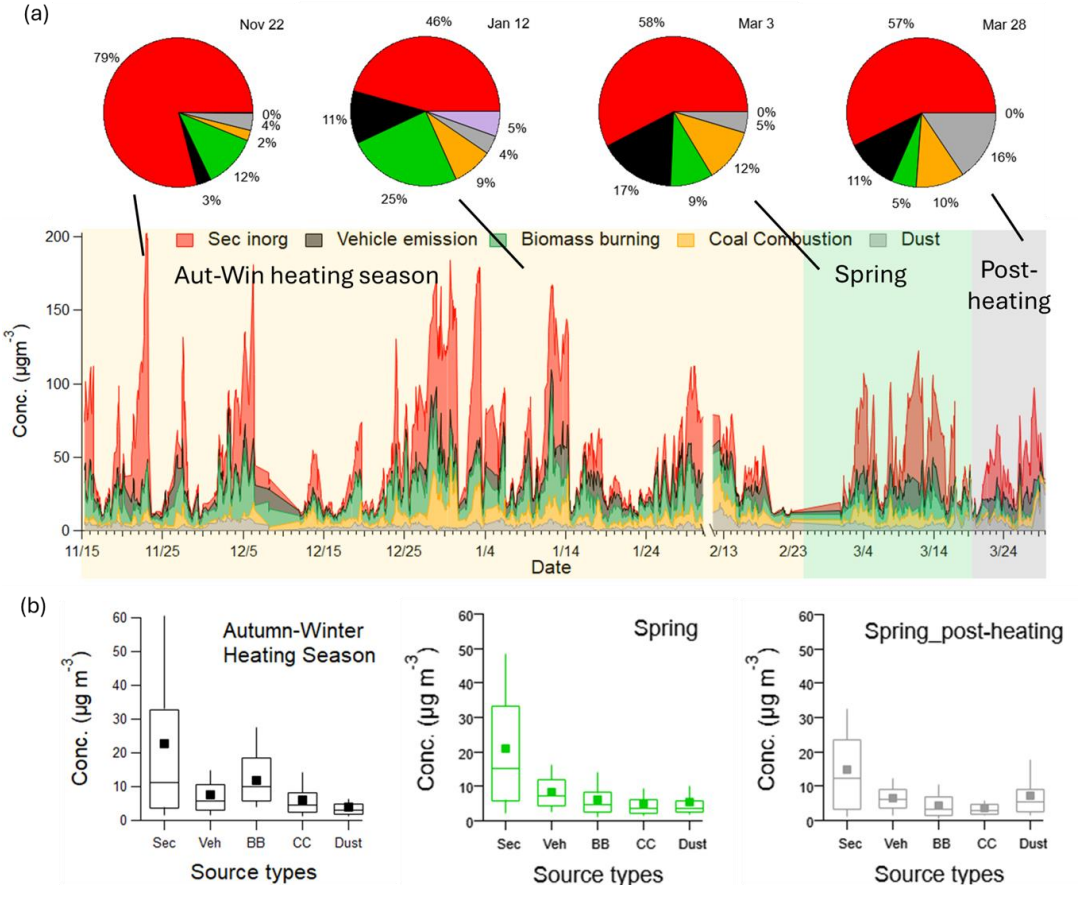

Figure 2. Source contribution variations during the sampling period, with pie charts showing four selected representative days (Nov 22, Jan 12, Mar 3, and Mar 28). Colors represent: red = secondary inorganic aerosols, black = vehicle emissions, green = biomass burning, orange = coal combustion, grey = dust, purple = others. (b) Concentrations of each identified source during the autumn-winter heating season, spring, and post-heating spring season. Abbreviations: Sec, secondary inorganic; Veh, vehicle emissions; BB, biomass burning; CC, coal combustion.

The diurnal profiles of the resolved source types reflected their inherent emission and atmospheric dynamics. Biomass burning exhibited a pronounced diurnal cycle, peaking at night (~15 μg m^{-3}) and reaching a minimum in the afternoon around 14:00 (<7 μg m^{-3}), coinciding with the maximum height of the typical urban boundary layer in NCP. In contrast, coal combustion peaked around 11:00, closely tracking the diurnal variations of SO_2 (Fig. S4). Given that residential coal combustion is the dominant source of SO_2 in this region,

https://doi.org/10.5194/egusphere-2026-4106
Preprint. Discussion started: 14 July 2026

this coherence confirms that the source apportionment successfully resolved coal combustion emissions. Vehicle emissions exhibited a higher contribution around 10 a.m., slightly earlier than coal combustion, aligning with the diurnal pattern of CO (Fig. S4). Similarly, NO_2 exhibited a morning enhancement; however, overall NO_2 concentrations were elevated at night due to reduced O_3 titration and additional nocturnal sources, such as biomass burning.

Regarding primary sources of $PM_{2.5}$ in Weifang, the whole sampling period can be divided into three phases: the autumn-winter heating season (Nov 15 – Feb 28), spring-heating season (Mar 1 – Mar 15), and the post-heating season (Mar 16 – Mar 19). Source apportionment with inorganic tracers revealed that secondary inorganic aerosols (SIA) peaked during the heating season, with a mean concentration of 23 μg m^{-3} and a 90th percentile reaching 67 μg m^{-3}. This is in contrast to spring, during which the 90th percentile dropped to 48 μg m^{-3} and further declined to 33 μg m^{-3} in the post-heating season, indicating that extreme pollution driven by secondary components in the heating season were largely mitigated in the non-heating season. During extremely polluted days, such as November 22 ($PM_{2.5}$: 136 μg m^{-3}) and January 12 (178 μg m^{-3}), secondary inorganics (79%) and solid fuel burning (36%) respectively dominated the pollution, with concentrations significantly higher than during the post-heating period. During the heating season, mean concentrations of biomass burning (15 μg m^{-3}) and coal combustion (8 μg m^{-3}) significantly exceeded spring season averages (6 μg m^{-3} for both). Conversely, dust contributions surged in the post-heating period, increasing from 3.9 μg m^{-3} (in the heating season) to 10 μg m^{-3}, driven by severe dust events in late March. On dust-impacted days (e.g., March 28), dust sources can elevate PM_{10} concentrations to over 660 μg m^{-3} while $PM_{2.5}$ remains below 50 μg m^{-3}, with most particles consisting of dust-derived $PM_{2.5}$ (>60%).

3.3 Sources of different OA compounds

We compared the correlations between identified OA compounds and different sources to further characterize the emission profiles, except for dust source that contributed little to OA (Fig. 3). The OA compounds most strongly correlated with coal combustion ($r > 0.75$) were characterized by high DBE values and a high proportion of S-containing compounds, albeit with relatively lower signal intensities (Fig. 3a). The S-containing compounds ($C_2H_4SO_4$, $C_3H_6SO_4$, and $C_9H_6SO_8$) were likely formed during coal burning, especially in the low-temperature residential burning process. During coal burning, the

https://doi.org/10.5194/egusphere-2026-4106
Preprint. Discussion started: 14 July 2026

content of sulfur containing groups (e.g., sulfone, sulfoxide, and sulfate) increased, likely because during coal combustions low-valence sulfur was oxidized to a high-valence state via radical and active oxygen reactions (Gao et al., 2022). During coal oxidation's initial stage, aliphatic and aromatic sulfur compounds decompose under oxygen exposure, generating sulfur radicals (C−S•) and sulfhydryl radicals (•SH). These radicals participate in key reactions to form H_2S, disulfide bonds (−S−S−), and sulfur-oxygen radicals (S−O•), which subsequently combine with oxygen species to produce sulfones or sulfoxides. Furthermore, certain high-DBE fragments (e.g., $C_9H_2O_6$ and C_5HNO_3; DBE/C: 0.78–1) are also found to correlate strongly with coal combustion, likely representing oxidized aromatic species (e.g., PAHs) or their combustion fragments (Fig. 3a). Despite having molecular weights under 400 Da, these ions may be generated from larger OA compounds via thermal fragmentation within the FIGAERO-CIMS (Stark et al., 2017).

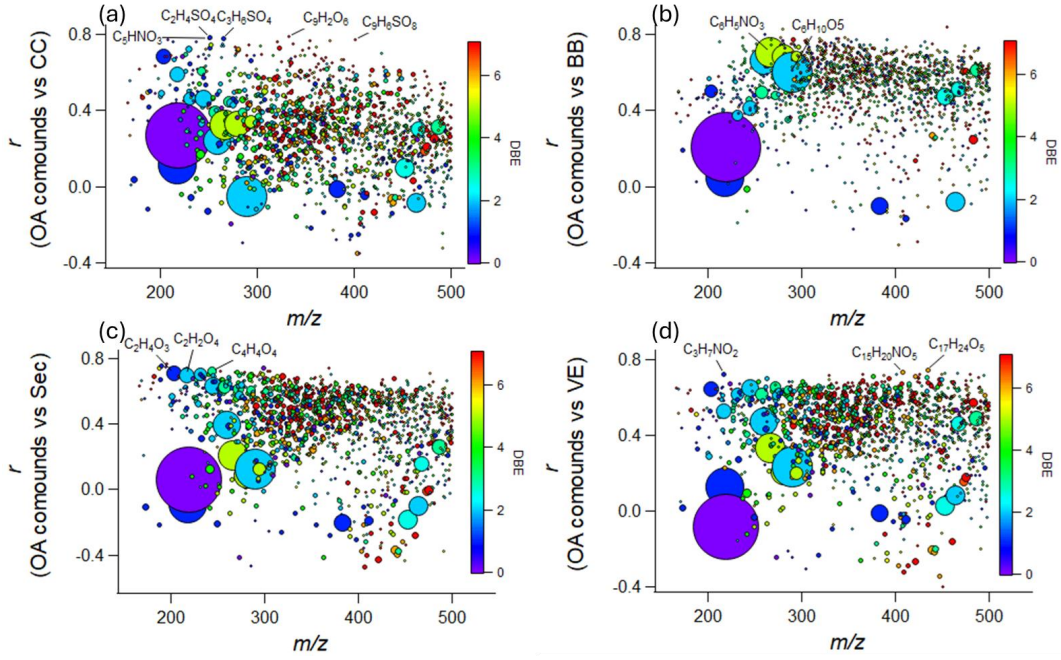

Figure 3. Correlation coefficients of compound concentrations and their correlations with different sources: (a) coal combustion, (b) biomass burning, (c) secondary inorganics, and (d) vehicle emissions. Dot sizes are proportional to the square root of the concentration for the corresponding compounds, and dots are color-coded by the DBE number of each compound. The two highest signal intensity compounds ($C_3H_8O_3$ and $C_3H_6O_3$) are likely thermal fragments of larger OA compounds.

https://doi.org/10.5194/egusphere-2026-4106
Preprint. Discussion started: 14 July 2026

Biomass burning-correlated species identified in the OA compounds included well-known tracers like levoglucosan ($C_6H_{10}O_5$, r = 0.63), nitrophenol ($C_6H_5NO_3$, r = 0.71), and nitrocatechol ($C_6H_5NO_4$, r = 0.72), which is shown in Fig. 3b. Nitrophenol derives were found to constitute ~1% of organic particulate matter in fresh biomass burning plumes (Mohr et al., 2013). Meanwhile, levoglucosan derives from crop residue cellulose degradation in high temperature (Cubison et al., 2011), and its moderate correlation with the biomass burning tracer can be explained by the co-emission of coal combustion alongside biomass burning in the NCP (Yan et al., 2017). During our sampling period, $C_6H_{10}O_5$ constituted ~0.9% of total OA, one in fourth of the levoglucosan-to-OA ratio in fresh biomass burning (~4%) (Mazzoleni et al., 2007), highlighting the significance of fresh biomass burning to ambient. Besides those widely reported tracers, compounds with 5 – 6 DBEs and molecular weights of 300 – 400 correlated strongly with biomass burning (Fig. 3b); these compounds likely represent one- or two-ring aromatics emitted during solid fuel burning activities. Compounds that were highly correlated with vehicle emissions showing higher molecular weight compounds (m/z > 350), moderate DBE/C ratios (~0.4) and were frequently N-containing (e.g., $C_{15}H_{20}NO_5$, $C_{17}H_{24}O_5$), pointing to oxidized organics from fuel combustion origins such as diesel traffic emissions (Fig. 3d, (Wang et al., 2022; Zhang et al., 2023)). Reactive nitrogen-containing organics emitted from vehicles may undergo hydrolysis and/or oxidation, forming the high-molecular-weight derivatives observed via methylation and hydroxylation. At night, these products react further with amine, nitro, and nitroso groups, while during the day, they undergo decarboxylation with the presence of hydroxyl radicals (•OH), further complicating the product mixture (Chen et al., 2025b).

Compounds strongly correlated with secondary inorganic sources exhibited low DBE values (1 – 3) and lower molecular masses (200 – 300 Da). Representative molecules ($C_2H_4O_3$, $C_2H_2O_4$, $C_4H_4O_4$) suggest low molecular weight organic acids or aldehydes (e.g., oxalic and maleic acid). Previous studies showed that these low organic acids attributed to aqueous heterogeneous reactions in the North China Plain, especially during haze or frog episode (Guo et al., 2010). These low-molecular-weight acids and diacids have been reported to be enriched in the condensation and droplet modes. They likely form via gas-phase photochemical processes and subsequently condense onto pre-existing particles. During haze events, high relative humidity (RH) further facilitates this condensation, thereby enhancing aerosol hygroscopic

https://doi.org/10.5194/egusphere-2026-4106
Preprint. Discussion started: 14 July 2026

growth and the enrichment of these compounds (Song et al., 2021). Beside those acids and diacids that are highly correlated, a large fraction of OA compounds from the mass range between 300 and 500 moderately correlated ($r = 0.4 - 0.5$) with the secondary inorganic factor, underscoring the importance and complex formation pathways of secondary formation as an OA source.

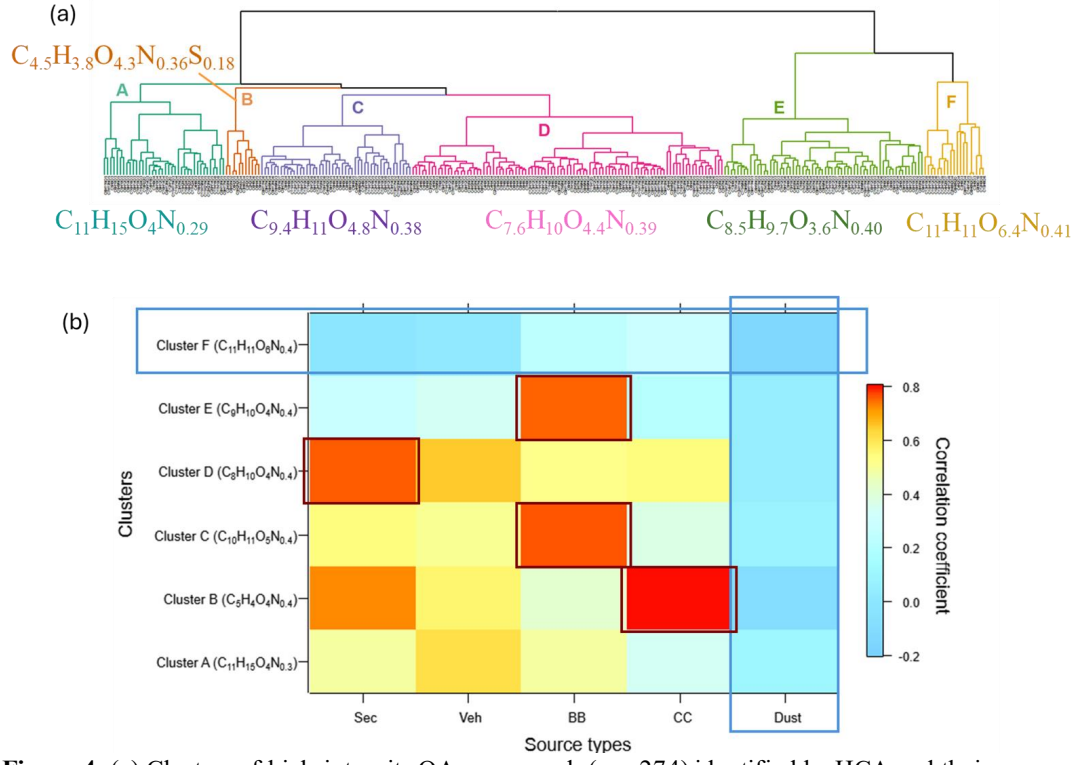

Figure 4. (a) Clusters of high-intensity OA compounds (n = 274) identified by HCA and their average molecular formula; (b) Spearman correlation coefficients between these clusters and PM sources resolved using the PMF method.

In order to characterize the variations of OA compounds, we selected high-abundance compounds that exhibited signal intensity higher than 0.05 % of the total CHOX signal and exceeded both field and instrument backgrounds by a factor of 2 (Cai et al., 2023), and then use the HCA method to cluster those high concentration compounds. Based on this criteria, 274 high-abundance compounds were selected and categorized into six clusters (Cluster A-F, Fig. 4a) using HCA method. The time series of these clusters were then correlated with the source apportionment results.

Cluster A compounds have an average formula of $C_{11}H_{15}O_4N_{0.3}$ and a low DBE/C ratio of 0.42. These compounds showed a moderate positive

https://doi.org/10.5194/egusphere-2026-4106
Preprint. Discussion started: 14 July 2026

correlation with secondary sources (r = 0.49 to 0.61), vehicle emissions, and biomass burning, but a negative correlation with coal combustion, suggesting they likely originate from the secondary formation or aging of vehicle emissions or biomass burning. In contrast, Cluster B compounds (average formula of $C_5H_4O_4N_{0.4}$) exhibited the highest DBE/C ratio of 1.0 among all clusters, indicating moderate oxidation and a highly aromatic-like character. This cluster was highly correlated with coal combustion (r = 0.81, Fig. 4b) and moderately correlated with secondary sources (r = 0.72), pointing to coal burning activities as its primary origin. Clusters C and E, with similar molecular formulae ($C_{10}H_{11}O_5N_{0.4}$ and $C_9H_{10}O_4N_{0.4}$, respectively) and identical DBE/C ratios (~0.57), were strongly positively correlated with biomass burning (r = 0.76, Fig. 4b) and negatively or weakly correlated with other sources (r = 0.0080 to 0.54). This suggests a biomass burning origin for both clusters, which is further supported by the presence of molecular markers such as levoglucosan and nitrocatechols in this cluster.

Cluster D, with an average formula of $C_8H_{10}O_4N_{0.4}$ and a low DBE/C ratio of 0.52 and a higher O:C ratio (0.70 ± 0.41), correlated with secondary inorganic sources (r = 0.75, Fig. 4b). This cluster contained the largest number of compounds (97 compounds, comprising 36% of the total high-intensity compounds). These compounds, which typically contain less than 8 carbon atoms, showed positive correlations with $PM_{2.5}$ (r = 0.87). They are likely low molecular weight, highly oxygenated molecules produced from fragmentation following prolonged photochemical processing or heterogenous reactions in haze events (Kroll et al., 2011). Finally, Cluster F showed negative or no correlation with all source types (Fig. 4b). This may be because some of these compounds, such as $C_3H_6O_3$ and $C_4H_2O_4$, are likely thermal fragments of larger OA compounds. These fragments are characterized by multiple peaks in their thermograms, with the most abundant signal occurring at 150 – 180 °C (Fig. S5), suggesting they likely originate from the thermal decomposition of a larger parent compound (Stark et al., 2017). Notably, dust source from PMF has no correlation with all OA compounds (r = -0.14 to 0.10, Fig. 4b) which makes sense since OA is more likely to come from combustion origins or secondary formation rather than dust in the NCP plain.

Overall, the consistent results and high correlation between the HCA-derived clusters and PMF-derived factors suggest that variations in the organic compounds measured by FIGAERO-CIMS in Weifang can be largely

https://doi.org/10.5194/egusphere-2026-4106
Preprint. Discussion started: 14 July 2026

explained by the identified $PM_{2.5}$ sources. This highlights that OA and $PM_{2.5}$ were dominated by common sources in Weifang, with secondary formation, biomass burning, coal combustion, and vehicle emissions acting as major contributors to both, whereas dust contributed exclusively to the inorganic fraction of PM during spring period.

3.4 OA compounds and sources driving OP_m and OP_v

In general, the OP_v levels in Weifang during the study period (average: 0.91 nmol min^{-1} m^{-3}; peak: 2.1 nmol min^{-1} m^{-3}) were comparable to the elevated OP_v levels reported in the rural NCP (Cao et al., 2025a), and were approximately twofold higher than those determined in Los Angeles (Shen et al., 2022). The correlation between OP_v and OC mass concentrations ($r = 0.80$) is significantly higher than those with transition metals such as iron (Fe, $r = 0.35$) or copper (Cu, $r = 0.56$), despite these metals typically being considered as one of the drivers of OP (Fig. S6) (Wang et al., 2020b; Charrier and Anastasio, 2012). When the firework case (Feb 11) is excluded, this correlation was further enhanced ($r = 0.85$), which underscores the dominant role of OC in driving the oxidative potential of $PM_{2.5}$ in Weifang.

The highest OP_v levels occurred during two distinct pollution episodes (Fig. 1b). On Jan 12, high secondary inorganic contribution (5%) and levoglucosan (0.59 µg m^{-3}; 1.9% of OA) indicated strong secondary formation and solid fuel burning contribution. In contrast, on Feb 11 (one day after Chinese New Year), firework emissions caused SO_2 and metals (Ba, Cu) to spike tenfold above the period average, driving OP_v to a comparable level (2.1 nmol min^{-1} m^{-3}). Despite the contrasting compound compositions and source profiles, similar OP_v values (2.1 nmol min^{-1} m^{-3}) were observed in these two episodes. Such a similarity indicates that OP driven by OA during biomass burning events could rival the toxicity levels driven by transition metals during firework events. To accurately compare OA activity, Feb 11 was excluded from further analysis, as its toxicity was dominated by firework metals rather than OA.

A small subset of OA compounds was found to be the key to driving the elevated intrinsic OP_m (Fig. S7). To further investigate those key compounds with molecular characteristics, we compared the average OP_v and OP_m with DBEs, O:C ratios, oxidation state, and carbon numbers across different compounds. In general, the correlation coefficient between OP_v and DBE enhanced significantly from 0.30 for saturated compounds (DBE = 0; e.g., polyols) to 0.80 for unsaturated species (DBE > 3, Fig. 5a). A slight reduction

https://doi.org/10.5194/egusphere-2026-4106
Preprint. Discussion started: 14 July 2026

in correlation at DBE = 5 is mainly attributed to nitrophenol. Although FIGAERO-CIMS is highly sensitive to these compounds (Zheng et al., 2021), the OP of 2-, 3-, and 4-nitrophenol isomers ranges from moderate to high (Khan et al., 2022). Consequently, this correlation drop likely reflects the contribution of lower-OP nitrophenol isomers. However, this general positive trend indicates that high-DBE compounds, likely aromatic derivatives, are major contributors to the OP_v of OA and $PM_{2.5}$ in Weifang.

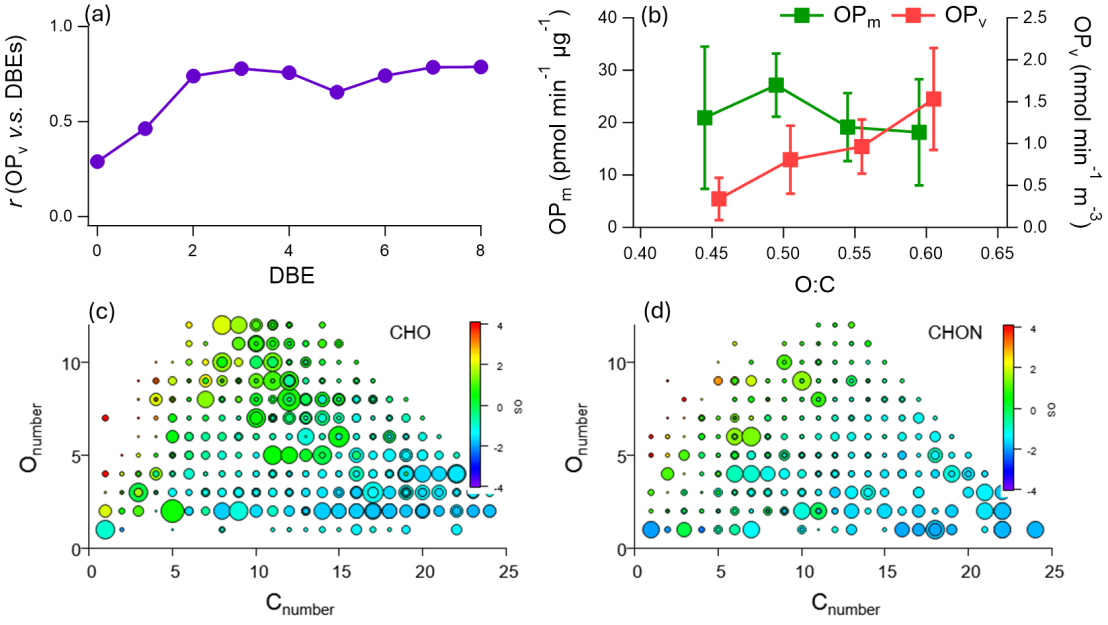

Figure 5. (a) Correlation coefficients between OP_v and the total signal for compounds with different DBEs; (b) OP_m and OP_v variation across different O:C ratio for CHO compounds (c) Spearman correlation coefficients between OP_m and the signal intensities of CHO compounds with varying O and C numbers. Compound markers are color-coded according to their average oxidation state; (d) Spearman correlation coefficients between OP_m and the signal intensities of CHON compounds with varying O and C numbers. Compound markers are color-coded according to their average oxidation state.

Interestingly, while OP_v continuously increased as the O:C ratio rose from 0.4 to 0.6, OP_m exhibited a diverging trend: it increased at lower O:C ratios but plateaued (~27 pmol min^{-1} μg^{-1}) or slightly decreased (~20 pmol min^{-1} μg^{-1}) when the O:C exceeded 0.5 (Fig. 5b). The continuous enhancement in OP_v with increasing O:C is likely driven by PM concentration; as PM levels increase, OA compounds become more aged and result in higher O:C ratio. However, the decline in OP_m at higher O:C implies that although initial oxidation enhances OA toxicity as widely reported in previous studies (Antiñolo et al., 2015); the highly oxygenated OA likely formed in the extremely haze periods

https://doi.org/10.5194/egusphere-2026-4106
Preprint. Discussion started: 14 July 2026

may exhibit lower OP activity in Weifang City, which is also validated by our test experiment using standard chemicals. Our findings are consistent with the spatial variations reported by Liu et al. (2024a), who showed that while highly oxygenated OA dominates OP activity in megacities like Beijing, primary emitted or moderately oxygenated OA compounds play a more important role in driving OP_m in rural areas of the NCP.

Moreover, we observed that compounds with the strongest positive correlations to OP_m generally exhibit moderate oxidation state OS_c (-1 to 1), with correlations decline significantly when OS_c exceeds 2. Highly oxygenated compounds (OS_c > 2), which primarily consist of <6 carbons and 2 – 10 oxygens, show weak or even negative correlations with OP_m. These compounds correspond predominantly to small-molecule carboxylic acids and aldehydes. In contrast, the most highly positive correlated OA compounds fall into two groups: (1) C_{10} – C_{15} with ~10 oxygen atoms and *m/z* around 300 (likely oxygenated aromatics linked to the solid fuel burning emissions in Section 3.3), and (2) long-chain species (> C_{15}) with less than 5 oxygen atoms. The latter group, particularly N-containing species with *m/z* > 350 and DBE of 5 – 6, likely represent oxidized traffic emissions as discussed in Section 3.3 and previous literature (Zhang et al., 2023; Chen et al., 2025b). This aligns with previous field observations in Europe, which identified Less-Oxygenated OOA (LO-OOA, particularly anthropogenic secondary OA), as a major contributor to OP activity, despite its much lower concentration compared to secondary inorganics (Daellenbach et al., 2020).

3.5 Apportioning the key sources of OP_m

To further illustrate the impacts of source to OP_m, we compare the source apportionment and corresponding OP_m variations during four episodes: Nov 22 ($PM_{2.5}$: 136 μg m^{-3}, OP_m: 28.7 pmol min^{-1} $μg^{-1}$), Jan 6 ($PM_{2.5}$: 68 μg m^{-3}, OP_m: 33.4 pmol min^{-1} $μg^{-1}$), Jan 21 ($PM_{2.5}$: 178 μg m^{-3}, OP_m: 36.8 pmol min^{-1} $μg^{-1}$), and Mar 28 ($PM_{2.5}$: 81 μg m^{-3}, OP_m: 26.8 pmol min^{-1} $μg^{-1}$). During the November 22 and March 28 episodes, secondary inorganic aerosols and dust were the dominant sources, comprising 76% and 47% of $PM_{2.5}$, respectively. However, their corresponding OP_m values (28.7 and 26.8 pmol min^{-1} $μg^{-1}$) were comparable to the campaign average (24 pmol min^{-1} $μg^{-1}$), implying that secondary inorganics and dust aerosols are not the key components driving of OP activity in Weifang city (Fig. 6a). In contrast, on January 6 and January 21, fine PM was dominated by biomass burning and coal combustion; together,

https://doi.org/10.5194/egusphere-2026-4106
Preprint. Discussion started: 14 July 2026

these two primary combustion sources accounted for up to 45% of the total mass, corresponding to the highest OP_m values observed across the four cases. On these two days, secondary OC accounted for approximately 40 – 60% of the total OC based on the OC/EC ratio method (Cao et al., 2007). These findings reinforce that primary solid fuel combustion and associated secondary organic aerosol formation are the dominant contributors to OP_m.

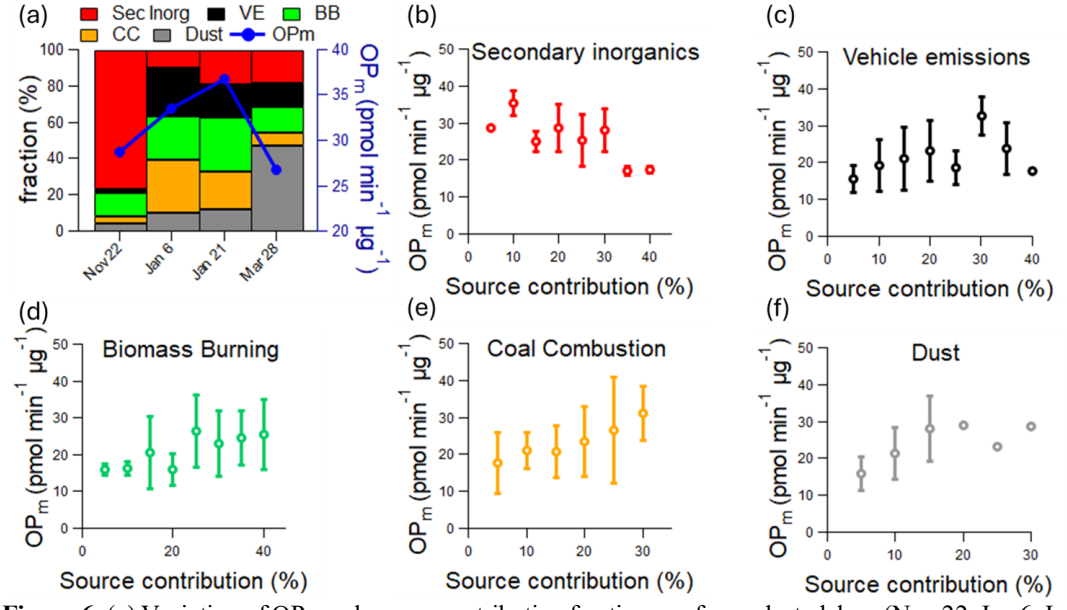

Figure 6. (a) Variation of OP_m and source contribution fractions on four selected days (Nov 22, Jan 6, Jan 21, and Mar 28). OP_m variations across the contributions of different source types: (b) secondary inorganics, (c) vehicle emissions, (d) biomass burning, (e) coal combustion, and (f) dust.

For the whole sampling period, OP_m generally declined as the contribution of secondary inorganics increased (Fig. 6b). The average value of OP_m dropped from 37 pmol min^{-1} μg^{-1} to as low as 17 pmol min^{-1} μg^{-1} when the contribution reached 40%. This trend is consistent with previous studies suggesting that a higher proportion of secondary inorganic component in the NCP may exert a dilution or suppression effect on the overall OP activity of $PM_{2.5}$ (Li et al., 2021). In contrast, OP_m initially increased with vehicle emissions but subsequently decreased below 20 pmol min^{-1} μg^{-1} once the vehicle contribution exceeded 20% – 30% (Fig. 6c). This decline is likely attributable to stagnant meteorological conditions during high-$PM_{2.5}$ episodes, which promote the concurrent accumulation of both vehicle emissions and secondary inorganic formations. Crucially, contributions from solid fuel (coal and biomass)

https://doi.org/10.5194/egusphere-2026-4106
Preprint. Discussion started: 14 July 2026

combustion showed a continuous positive relationship with OP_m, with this enhancing effect persisting up to 40% contribution (Fig. 6d and 6e), which underscores the important role of solid fuel burning in driving OP_m. On the other hand, OP_m associated with dust increased to 28 pmol min^{-1} μg^{-1} as its contribution rose from 5% to 15% but stabilized or even decreased to 23 pmol min^{-1} μg^{-1} beyond 15% (Fig. 6f). This suggests that pure dust is not a major driver of OP_m, owing to the low solubility of crustal metals. Nevertheless, a previous study showed that the solubility and toxicity of dust aerosols could increase significantly when they are transported over polluted regions and mix with anthropogenic emissions in NCP (Zhang et al., 2026).

To quantitatively identify the key OP-active compounds and their dominant sources, a multilinear regression (MLR) model was applied to the time series to apportion the contribution of individual compound among the four OA sources identified via cluster analysis: secondary inorganics, biomass burning, vehicle emissions, and coal combustion. Consistent with the HCA analysis, key OP-active compounds were selected based on a significant correlation with OP_m (t-test, $p < 0.05$) among 274 high-signal-intensity compounds (signal intensity > 0.05% of CHOX).

The regression coefficients derived from the MLR model for each compound across the four sources were extracted and normalized to their respective maximum coefficients. These normalized coefficients for the most positive and negative correlated compound are shown in Fig. 7a and b, respectively, alongside the temporal variations and OP_m correlation coefficients of each compound. Accordingly, for compounds positively correlated with OP_m, a higher regression coefficient for a specific source indicates that the source is the primary contributor to the compound, thereby exerting a significant positive influence on the overall OP. Conversely, for compounds negatively correlated with OP_m, a higher regression coefficient suggests that whereas the source dominates the compound's abundance, it likely exerts a negligible or suppressive effect on the OP_m of total $PM_{2.5}$.

It was found that only a small fraction of high-intensity compounds was positively correlated with measured OP_m (72 out of 274 species), indicating that a minority of high-abundance compounds drive OA toxicity. Concurrently, these OP-active species showed a strong negative correlation with secondary inorganic sources (t-test, $p < 0.05$). Furthermore, the compounds significantly correlated with OP_m ($r > 0.4$) exhibited a high average DBE of 6.4 ± 4.2 and

https://doi.org/10.5194/egusphere-2026-4106
Preprint. Discussion started: 14 July 2026

an O:C ratio of 0.72 ± 0.36, the latter of which was primarily attributed to the species containing high oxygen number (typically associated with primary sources, especially biomass burning and coal combustion). Representative examples include high-DBE species linked to coal combustion (e.g., $C_{15}H_6O_6$ and $C_{12}H_8O_8$), biomass burning related molecules (e.g., $C_{15}H_{12}O_8$ and $C_{15}H_{14}O_8$), and vehicle-derived emission characterized by nitro-aromatic compounds and high molecular-weight compounds (e.g., $C_6H_6N_2O_2$ and $C_{14}H_{28}O_7$).

Notably, these high-DBE compounds, likely aromatics with multiple carbon rings, typically feature multiple hydroxyl groups and conjugated systems, which confer strong electron-donating capacity and enable the generation of reactive oxygen species, such as singlet oxygen ($^1O_2$) and superoxide anion ($\bullet O_2^-$). Beyond possessing high intrinsic oxidative potential, these polycyclic aromatic compounds can catalyze transition metal cycling in Fenton-like systems, which further boosts ROS generation (Cao et al., 2025b; Yu et al., 2022). Additionally, nitro-derivatives of these aromatic compounds not only exhibit intrinsic redox activity but also exacerbate oxidative stress by undergoing single-electron reduction to form $\bullet NO_2$, subsequently initiating lipid peroxidation and contributing to elevated OP_m (Cao et al., 2026). Aromatic amines, such as the nitroanilines ($C_6H_6N_2O_2$) found in this study (average concentration of 3.6 ng m^{-3}), may promote the formation of electrophilic reactive intermediates capable of interacting with DNA, thereby leading to severe genotoxicity (Zhang et al., 2025).

Under the low temperature and low relative humidity environment that typically predominant the NCP during autumn and winter, aromatic compounds tend to stabilize their benzene ring structures under such conditions (Cao et al., 2026). As a result, they predominantly undergo "ring-preserving" rather than "ring-opening" reactions during atmospheric aging, which allows them to maintain high toxicity after transport and aging process (Kautzman et al., 2010). Furthermore, the acidic aerosol environment (Cheng et al., 2016) in the NCP may further increase molar yields of ROS species (e.g., H_2O_2) within SOA, driven by accelerated α-hydroxyhydroperoxide decomposition and quinone redox cycling (Wei et al., 2022). These findings underscore the significant contribution of OP-active compounds from primary emissions and subsequent oxidation in Weifang and broader NCP region.

https://doi.org/10.5194/egusphere-2026-4106
Preprint. Discussion started: 14 July 2026

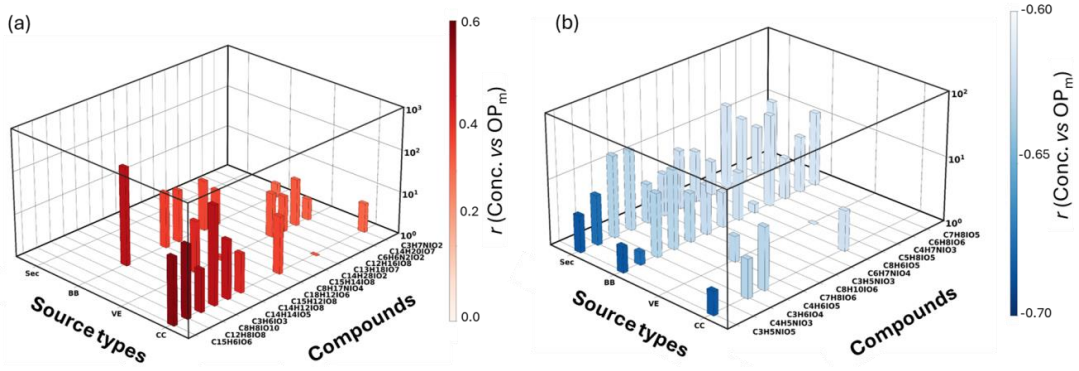

Figure 7. Correlation coefficients of compounds that are significantly correlated with OP_m: (a) positively correlated compounds and (b) negatively correlated compounds. The compounds are plotted based on the normalized coefficients in the multi-linear regression model for each source type and are color-coded by their correlation coefficient with OP_m.

Most of high signal intensity OA compounds showed a negative correlation with OP_m (202 out of 274 species). Specifically, we investigated those exhibiting strong negative correlations with OP (r < -0.6), which were characterized by a lower DBE (3.0 ± 1.3), a significantly higher O:C ratio (0.75 ± 0.35), and an average molecular formula of $C_{5.2}H_{6.8}O_{4.6}N_{0.38}$. Prominent compounds in this group included glyceric acid ($C_3H_6O_4$), malic acid ($C_4H_6O_5$), and $C_5H_8O_5$ (likely hydroxyglutaric acid). Glyceric and malic acids are mainly formed via heterogeneous or liquid-phase reactions that are typically enhanced during haze episodes, whereas $C_5H_8O_5$ is a well-known SOA product derived from isoprene oxidation (Claeys et al., 2007) and tends to possess lower OP (Tuet et al., 2017). To verify these field-derived findings, laboratory OP tests of authentic standards were conducted, which further corroborated the low redox activity of these compounds (Fig. 8). Specifically, despite their relatively high abundance in OA during sampling period, glyceric acid ($C_3H_6O_4$, average: 84 ± 10 ng m^{-3}) and malic acid ($C_4H_6O_5$, average: 90 ± 10 ng m^{-3}) exhibited negligible intrinsic OP_m values (8.8 and 22 pmol min^{-1} μg^{-1}, respectively). These levels are comparable to those of low-activity inorganics such as ammonium sulfate (13 ± 6.9 pmol min^{-1} μg^{-1}) and ammonium nitrate (5.1 ± 3.5 pmol min^{-1} μg^{-1}).

https://doi.org/10.5194/egusphere-2026-4106
Preprint. Discussion started: 14 July 2026

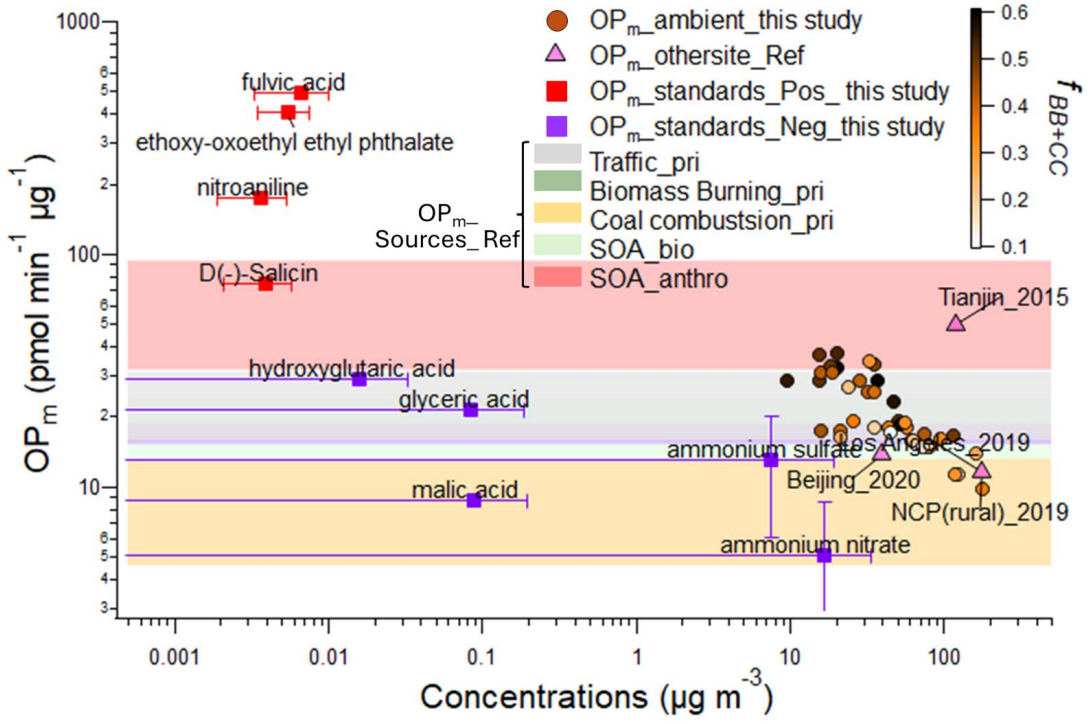

Figure 8. Mass-normalized oxidative potential (OP_m) derived from offline samples and chemical standards in the study. Offline samples collected during the campaign are represented by brown circles, color-coded according to the fractional contribution of solid fuel (biomass burning plus coal combustion). OP_m data previously measured in the NCP are shown in pink triangles, including Beijing in 2020 (Li et al., 2024; Zheng et al., 2026), Tianjin in 2015 (Liu et al., 2018) and NCP rural area in 2019 (Liu et al., 2024b). Chemical standards measured in this study are shown as squares, with red and purple representing compounds positively and negatively correlated with OP, respectively, and error bars represent the standard deviations. Additionally, the standard deviation ranges of previously reported OP_m values from various sources are illustrated using different color shades. These include primary OP_m from traffic (Traffic_pri), biomass burning (Biomass_burning_pri), and coal combustion (Coal_combustion_pri), as well as SOA from biogenic precursors (SOA_bio) and from two aromatic precursors (m-xylene and naphthalene). The data sources are derived from the following references: Liu et al. (2024b); Bates et al. (2019) Cheung et al. (2010); Fushimi et al. (2017); Jiang et al. (2016); Mcwhinney et al. (2013); Tuet et al. (2017)

To evaluate the potential redox activity of the molecular formulas significantly and positively correlated with OP_m, such as $C_{14}H_{12}O_8$, $C_{13}H_{18}O_7$, $C_{14}H_{14}O_5$, and $C_6H_6N_2O_2$, we also conducted OP tests using commercially available standards as representative surrogates (Fig. 8). Notably, these tested isomers (fulvic acid, D(-)-salicin, ethoxycarbonylmethyl ethyl phthalate, and nitroaniline) exhibited exceptionally high intrinsic OP_m values (75 – 490 pmol min^{-1} μg^{-1}), which is about 3 to 23 times greater than the ambient average (22 pmol min^{-1} μg^{-1}). Moreover, the OP_m of these tested species substantially

https://doi.org/10.5194/egusphere-2026-4106
Preprint. Discussion started: 14 July 2026

exceeded those of transition metals reported in the literature (e.g., Cu: 32 pmol min^{-1} μg^{-1}; V: 20 pmol min^{-1} μg^{-1}; Fig. S8).

Most ambient samples exhibited OP_m values significantly higher than those of biogenic SOA (e.g., isoprene: 10 ± 2 pmol min^{-1} μg^{-1}; α-pinene: 25 ± 7 pmol min^{-1} μg^{-1}), but fell within the range of anthropogenic SOA derived from aromatics (e.g., m-xylene: 24 ± 11 pmol min^{-1} μg^{-1}; naphthalene: 150 ± 50 pmol min^{-1} μg^{-1}). Notably, we observed that OP_m scaled positively with the fractional contribution of solid fuel combustion (biomass and coal). In particular, samples with the highest OP_m had solid fuel combustion fractions exceeding 50%. Their OP_m values surpassed previously reported ranges for primary PM from coal combustion, biomass burning, and vehicle emissions, reaching levels typical of anthropogenic aromatic SOA. Given that primary OA alone cannot account for these elevated OP_m values, and that OP-active compounds in Weifang are generally moderately oxygenated, we infer that moderately oxygenated anthropogenic OA, specifically aged primary OA, plays a critical role in driving OP activity in the NCP.

The lowest OP_m observed in Weifang (~10 pmol min^{-1} μg^{-1}) aligns well with 2019 rural NCP data (Liu et al., 2024b) and our previously reported average (~14 pmol min^{-1} μg^{-1}) observed in Beijing in 2020, where residential burning was strictly regulated. In contrast, the highest OP_m in our study (38 pmol min^{-1} μg^{-1}) approaches the level in Tianjin in 2015 (49 pmol min^{-1} μg^{-1}) when the initial implementation of the Air Pollution Prevention and Control Action Plan. These comparisons highlight that even under regionally homogeneous PM concentrations, OP activity varies drastically across the NCP depending on emission sources. This underscores an urgent need for targeted pollution control beyond megacities, particularly regarding solid fuel burning emissions, especially in medium- and small-sized cities where the majority of the NCP population resides.

4. Conclusions

Whereas effective air pollution controls have significantly reduced $PM_{2.5}$ levels across China (e.g., from 72 to 35 μg m^{-3} between 2013 and 2020 in 74 key cities (Chen et al., 2024)), the relative contribution of OA, particularly SOA, has increased. Unlike Beijing, where primary emissions are continuously declining, medium- and small-sized NCP cities like Weifang still suffer from severe PM pollution, particularly during the heating season. Molecular-level

https://doi.org/10.5194/egusphere-2026-4106
Preprint. Discussion started: 14 July 2026

investigation in this study revealed that OP was crucially affected by OA in Weifang, which was substantially associated with solid fuel burning tracers. These included tracer molecules from coal combustion (e.g., $C_{15}H_6O_6$ and $C_{12}H_8O_8$) and biomass burning (e.g., $C_{15}H_{12}O_8$ and $C_{15}H_{14}O_8$), alongside high-molecular-weight, low-DBE nitro-aromatics likely from vehicle emissions (e.g., $C_6H_6N_2O_2$ and $C_{14}H_{28}O_7$). Conversely, most OA compounds were only moderately correlated with OP_m, indicating a potentially moderate contribution to OP_m but an evident cumulative contribution to OP_v. Some highly oxygenated, low-molecular-weight OA species, such as small-molecule carboxylic acids (e.g., malic and glyceric acid) that are strongly correlated with secondary inorganics and are likely to form during haze episodes, probably contribute little to the overall OP.

Cluster and multilinear regression analyses further demonstrate that solid fuel combustion (biomass and coal) substantially drives high OP activity, while secondary inorganics negatively impact OP_m. Still, we note that our online PMF and offline FIGAERO-CIMS analyses using HCA and MLR methods cannot fully separate primary emissions from their subsequent aging processes. The fact that the high fraction of SOA and high OP_m cannot be explained by primary emissions alone suggests that, in addition to primary sources, post-emission oxidation following fuel burning is also crucial to OP activity during the heating season in Weifang.

Our findings show that OP activity may vary significantly across the NCP region, especially between megacities (e.g., Beijing) and medium-sized cities (e.g., Weifang) due to substantially different OA composition and origins. This underscores the continued need for primary emission controls, particularly those targeting solid fuels, such as the implementation of coal-to-gas switching policies in the broader NCP region. Given the large populations in these cities and the strong OP activity linked to solid fuel combustion, such measures would greatly benefit public health.

Author Contributions

JC, XF, and M.L. designed the research. JC and XF analyzed the FIGAERO-CIMS data and interpreted the results. JC and FZ conducted PMF and HCA analyses. YZ, LS, RL, and LW provided online $PM_{2.5}$ chemical composition data. DD and JW provided the emission inventory for the NCP region. YL, CL, and WD provided valuable discussions and suggestions. JC, XF, QZ, and ML wrote the manuscript with contributions from all co-authors. All authors have read and approved the final version of the manuscript.

https://doi.org/10.5194/egusphere-2026-4106
Preprint. Discussion started: 14 July 2026

Data Availability

Data used in figures are available from the Zenodo online repository (DOI https://zenodo.org/records/21298413, Cai, 2026). Supporting data are available from the authors upon request.

Acknowledgement

This work was supported through the National Natural Science Foundation of China (Grants 42422505), the Jiangsu Specially Appointed Professor (R2025T01), the National Key Research and Development Program (2022YFC3700304). The authors thank the Open Grants of the China Meteorological Administration Aerosol-Cloud and Precipitation Key Laboratory (KDW2409) and Chengdu Plain Urban Meteorology and Environment Observation and Research Station of Sichuan Province (CPUME202407) and Shandong Provincial Natural Science Foundation (No. ZR2024QB339) for funding.

References

Antiñolo, M., Willis, M. D., Zhou, S., and Abbatt, J. P. D.: Connecting the oxidation of soot to its redox cycling abilities, Nature Communications, 6, 10.1038/ncomms7812, 2015.

Bates, J. T., Fang, T., Verma, V., Zeng, L., Weber, R. J., Tolbert, P. E., Abrams, J. Y., Sarnat, S. E., Klein, M., Mulholland, J. A., and Russell, A. G.: Review of Acellular Assays of Ambient Particulate Matter Oxidative Potential: Methods and Relationships with Composition, Sources, and Health Effects, Environmental Science & Technology, 53, 4003-4019, 10.1021/acs.est.8b03430, 2019.

Cai, J., Daellenbach, K. R., Wu, C., Zheng, Y., Zheng, F., Du, W., Haslett, S. L., Chen, Q., Kulmala, M., and Mohr, C.: Characterization of offline analysis of particulate matter with FIGAERO-CIMS, Atmospheric Measurement Techniques, 16, 1147-1165, 10.5194/amt-16-1147-2023, 2023.

Cai, J., Wu, C., Wang, J., Du, W., Zheng, F., Hakala, S., Fan, X., Chu, B., Yao, L., Feng, Z., Liu, Y., Sun, Y., Zheng, J., Yan, C., Bianchi, F., Kulmala, M., Mohr, C., and Daellenbach, K. R.: Influence of organic aerosol molecular composition on particle absorptive properties in autumn Beijing, Atmospheric Chemistry and Physics, 22, 1251-1269, 10.5194/acp-22-1251-2022, 2022.

Cao, F., Chen, Y., Han, Y., Chen, T., Feng, X., Jiang, H., Zhang, Q., Ma, H., Li, J., and Zhang, G.: Key toxicity enhancement effect of aqueous-phase secondary formation: Insights from hourly measurements during haze events, Journal of Hazardous Materials, 492, 10.1016/j.jhazmat.2025.138139, 2025a.

Cao, F., Feng, X., Han, Y., Chen, Y., Jiang, H., Chen, T., Shang, Y., Peng, Y., Liu, Z., Cai, J., and Li, D.: Dynamic oxidative potential of organic matter and their source-specific key toxicants during haze episodes in North China, Environment International, 209, 10.1016/j.envint.2026.110166, 2026.

Cao, F., Feng, X., Chen, Y., Jiang, H., Han, Y., Chen, T., Shang, Y., Li, D., Zhang, Q., Ma, H., Li, J., and Zhang, G.: Oxygenated aromatic compounds as dominant contributors to the oxidative potential of PM2.5 emitted from biomass burning and coal combustion, Journal of Hazardous Materials, 498, 10.1016/j.jhazmat.2025.139902, 2025b.

https://doi.org/10.5194/egusphere-2026-4106
Preprint. Discussion started: 14 July 2026

Cao, J. J., Lee, S. C., Chow, J. C., Watson, J. G., Ho, K. F., Zhang, R. J., Jin, Z. D., Shen, Z. X., Chen, G. C., Kang, Y. M., Zou, S. C., Zhang, L. Z., Qi, S. H., Dai, M. H., Cheng, Y., and Hu, K.: Spatial and seasonal distributions of carbonaceous aerosols over China, Journal of Geophysical Research: Atmospheres, 112, 10.1029/2006jd008205, 2007.

Charrier, J. G. and Anastasio, C.: On dithiothreitol (DTT) as a measure of oxidative potential for ambient particles: evidence for the importance of soluble transition metals, Atmospheric Chemistry and Physics, 12, 9321-9333, 10.5194/acp-12-9321-2012, 2012.

Chen, L., Liu, C., Wang, J., Chen, G., Zhao, Y., Jin, Y., and Jin, H.: How is the spatiotemporal representativeness of ground- and satellite-based aerosol optical depth (AOD) measurements over Asia?, Atmospheric Research, 315, 10.1016/j.atmosres.2024.107857, 2025a.

Chen, Q., Miao, R., Geng, G., Shrivastava, M., Dao, X., Xu, B., Sun, J., Zhang, X., Liu, M., Tang, G., Tang, Q., Hu, H., Huang, R.-J., Wang, H., Zheng, Y., Qin, Y., Guo, S., Hu, M., and Zhu, T.: Widespread 2013-2020 decreases and reduction challenges of organic aerosol in China, Nature Communications, 15, 4465, 10.1038/s41467-024-48902-0, 2024.

Chen, Q. C., Wang, M. M., Wang, Y. Q., Zhang, L. X., Li, Y. G., and Han, Y. M.: Oxidative Potential of Water-Soluble Matter Associated with Chromophoric Substances in PM2.5 over Xi'an, China, ENVIRONMENTAL SCIENCE & TECHNOLOGY, 53, 8574-8584, 10.1021/acs.est.9b01976, 2019.

Chen, S., Xu, Y., Liu, D., Deng, J., Liu, R., Kong, S., and Fu, P.: High chemodiversity of nitrogen-containing organic compounds in vehicle emissions driven by transformative reactions, Journal of Hazardous Materials, 495, 10.1016/j.jhazmat.2025.138803, 2025b.

Chen, X., Li, K., Bian, H., Zhang, S., Ma, X., Fang, L., Jiang, W., Yan, C., and Du, L.: Monoterpenes amplify the oxidative potential of biomass burning secondary aerosols, Journal of Hazardous Materials, 501, 10.1016/j.jhazmat.2025.140950, 2026.

Cheng, Y., Zheng, G., Wei, C., Mu, Q., Zheng, B., Wang, Z., Gao, M., Zhang, Q., He, K., Carmichael, G., Pöschl, U., and Su, H.: Reactive nitrogen chemistry in aerosol water as a source of sulfate during haze events in China, Science Advances, 2, e1601530, doi:10.1126/sciadv.1601530, 2016.

Cheung, K., Ntziachristos, L., Tzamkiozis, T., Schauer, J. J., Samaras, Z., and Moore, K. F.: Emissions of Particulate Trace Elements, Metals and Organic Species from Gasoline, Diesel, and Biodiesel Passenger Vehicles and Their Relation to Oxidative Potential, Aerosol Science and Technology, 44, 500-513, 10.1080/02786821003758294, 2010.

Cho, A. K., Sioutas, C., Miguel, A. H., Kumagai, Y., Schmitz, D. A., Singh, M., Eiguren-Fernandez, A., and Froines, J. R.: Redox activity of airborne particulate matter at different sites in the Los Angeles Basin, Environmental Research, 99, 40-47, https://doi.org/10.1016/j.envres.2005.01.003, 2005.

Claeys, M., Szmigielski, R., Kourtchev, I., Van der Veken, P., Vermeylen, R., Maenhaut, W., Jaoui, M., Kleindienst, T. E., Lewandowski, M., Offenberg, J. H., and Edney, E. O.: Hydroxydicarboxylic Acids: Markers for Secondary Organic Aerosol from the Photooxidation of α-Pinene, Environmental Science & Technology, 41, 1628-1634, 10.1021/es0620181, 2007.

Cubison, M. J., Ortega, A. M., Hayes, P. L., Farmer, D. K., Day, D., Lechner, M. J., Brune, W. H., Apel, E., Diskin, G. S., Fisher, J. A., Fuelberg, H. E., Hecobian, A., Knapp, D. J., Mikoviny, T., Riemer, D., Sachse, G. W., Sessions, W., Weber, R. J., Weinheimer, A. J., Wisthaler, A., and Jimenez, J. L.: Effects of aging on organic aerosol from open biomass burning smoke in aircraft and laboratory studies, Atmospheric Chemistry and Physics, 11, 12049-12064, 10.5194/acp-11-12049-2011, 2011.

Daellenbach, K. R., Uzu, G., Jiang, J., Cassagnes, L. E., Leni, Z., Vlachou, A., Stefenelli, G., Canonaco, F., Weber, S., Segers, A., Kuenen, J. J. P., Schaap, M., Favez, O., Albinet, A., Aksoyoglu, S., Dommen, J., Baltensperger, U., Geiser, M., El Haddad, I., Jaffrezo, J. L., and Prevot, A. S. H.: Sources of particulate-matter air pollution and its oxidative potential in Europe, Nature, 587, 414-419, 10.1038/s41586-020-2902-8, 2020.

https://doi.org/10.5194/egusphere-2026-4106
Preprint. Discussion started: 14 July 2026

Dai, Q., Chen, J., Wang, X., Dai, T., Tian, Y., Bi, X., Shi, G., Wu, J., Liu, B., Zhang, Y., Yan, B., Kinney, P. L., Feng, Y., and Hopke, P. K.: Trends of source apportioned PM2.5 in Tianjin over 2013–2019: Impacts of Clean Air Actions, Environmental Pollution, 325, 10.1016/j.envpol.2023.121344, 2023.

Dou, J., Lin, P., Kuang, B.-Y., and Yu, J. Z.: Reactive Oxygen Species Production Mediated by Humic-like Substances in Atmospheric Aerosols: Enhancement Effects by Pyridine, Imidazole, and Their Derivatives, Environmental Science & Technology, 49, 6457-6465, 10.1021/es5059378, 2015.

Fang, T., Lakey, P. S. J., Weber, R. J., and Shiraiwa, M.: Oxidative Potential of Particulate Matter and Generation of Reactive Oxygen Species in Epithelial Lining Fluid, Environmental Science & Technology, 53, 12784-12792, 10.1021/acs.est.9b03823, 2019.

Fushimi, A., Saitoh, K., Hayashi, K., Ono, K., Fujitani, Y., Villalobos, A. M., Shelton, B. R., Takami, A., Tanabe, K., and Schauer, J. J.: Chemical characterization and oxidative potential of particles emitted from open burning of cereal straws and rice husk under flaming and smoldering conditions, Atmospheric Environment, 163, 118-127, 10.1016/j.atmosenv.2017.05.037, 2017.

Gao, F., Jia, Z., Shan, Y.-f., Teng, Y., Li, Y.-d., and Pu, X.-g.: Influence of Organic Sulfur on Low-Temperature Oxidation of Coal and its Transition Characteristics, ACS Omega, 7, 39830-39839, 10.1021/acsomega.2c03824, 2022.

Geng, G., Liu, Y., Liu, Y., Liu, S., Cheng, J., Yan, L., Wu, N., Hu, H., Tong, D., Zheng, B., Yin, Z., He, K., and Zhang, Q.: Efficacy of China's clean air actions to tackle PM2.5 pollution between 2013 and 2020, Nature Geoscience, 17, 987-994, 10.1038/s41561-024-01540-z, 2024.

Gu, Y., Huang, R.-J., Duan, J., Xu, W., Lin, C., Zhong, H., Wang, Y., Ni, H., Liu, Q., Xu, R., Wang, L., and Li, Y. J.: Multiple pathways for the formation of secondary organic aerosol in the North China Plain in summer, Atmospheric Chemistry and Physics, 23, 5419-5433, 10.5194/acp-23-5419-2023, 2023.

Guo, S., Hu, M., Wang, Z. B., Slanina, J., and Zhao, Y. L.: Size-resolved aerosol water-soluble ionic compositions in the summer of Beijing: implication of regional secondary formation, Atmos. Chem. Phys., 10, 947-959, 10.5194/acp-10-947-2010, 2010.

Hu, J., Wang, Y., Ying, Q., and Zhang, H.: Spatial and temporal variability of PM2.5 and PM10 over the North China Plain and the Yangtze River Delta, China, Atmospheric Environment, 95, 598-609, 10.1016/j.atmosenv.2014.07.019, 2014.

Huang, R. J., Zhang, Y., Bozzetti, C., Ho, K. F., Cao, J. J., Han, Y., Daellenbach, K. R., Slowik, J. G., Platt, S. M., Canonaco, F., Zotter, P., Wolf, R., Pieber, S. M., Bruns, E. A., Crippa, M., Ciarelli, G., Piazzalunga, A., Schwikowski, M., Abbaszade, G., Schnelle-Kreis, J., Zimmermann, R., An, Z., Szidat, S., Baltensperger, U., El Haddad, I., and Prevot, A. S.: High secondary aerosol contribution to particulate pollution during haze events in China, Nature, 514, 218-222, 10.1038/nature13774, 2014.

Jia, Y., Rahn, K. A., He, K., Wen, T., and Wang, Y.: A novel technique for quantifying the regional component of urban aerosol solely from its sawtooth cycles, Journal of Geophysical Research, 113, 10.1029/2008jd010389, 2008.

Jiang, H., Jang, M., Sabo-Attwood, T., and Robinson, S. E.: Oxidative potential of secondary organic aerosols produced from photooxidation of different hydrocarbons using outdoor chamber under ambient sunlight, Atmospheric Environment, 131, 382-389, 10.1016/j.atmosenv.2016.02.016, 2016.

Kautzman, K. E., Surratt, J. D., Chan, M. N., Chan, A. W. H., Hersey, S. P., Chhabra, P. S., Dalleska, N. F., Wennberg, P. O., Flagan, R. C., and Seinfeld, J. H.: Chemical Composition of Gas- and Aerosol-Phase Products from the Photooxidation of Naphthalene, The Journal of Physical Chemistry A, 114, 913-934, 10.1021/jp908530s, 2010.

Khan, F., Jaoui, M., Rudziński, K., Kwapiszewska, K., Martinez-Romero, A., Gil-Casanova, D., Lewandowski, M., Kleindienst, T. E., Offenberg, J. H., Krug, J. D., Surratt, J. D., and Szmigielski, R.: Cytotoxicity and oxidative stress induced by atmospheric mono-nitrophenols in human lung cells, Environmental Pollution, 301, 10.1016/j.envpol.2022.119010, 2022.

https://doi.org/10.5194/egusphere-2026-4106
Preprint. Discussion started: 14 July 2026

Kroll, J. H., Donahue, N. M., Jimenez, J. L., Kessler, S. H., Canagaratna, M. R., Wilson, K. R., Altieri, K. E., Mazzoleni, L. R., Wozniak, A. S., Bluhm, H., Mysak, E. R., Smith, J. D., Kolb, C. E., and Worsnop, D. R.: Carbon oxidation state as a metric for describing the chemistry of atmospheric organic aerosol, Nature Chemistry, 3, 133-139, 10.1038/nchem.948, 2011.

Kulmala, M., Kokkonen, T. V., Pekkanen, J., Paatero, S., Petäjä, T., Kerminen, V.-M., and Ding, A.: Opinion: Gigacity – a source of problems or the new way to sustainable development, Atmospheric Chemistry and Physics, 21, 8313-8322, 10.5194/acp-21-8313-2021, 2021.

Li, J., Hua, C., Ma, L., Chen, K., Zheng, F., Chen, Q., Bao, X., Sun, J., Xie, R., Bianchi, F., Kerminen, V.-M., Petäjä, T., Kulmala, M., and Liu, Y.: Key drivers of the oxidative potential of PM2.5 in Beijing in the context of air quality improvement from 2018 to 2022, Environment International, 187, 10.1016/j.envint.2024.108724, 2024.

Li, S., Zhou, R., Wu, W., Luan, M., Li, X., Liu, C., Zhang, L., Liu, Y., Tan, F., Han, X., Wang, Q., Tan, J., Zou, Y., Yu, L., and Li, W.: Fine particulate matter induces cardiac fibrosis via the CHOP/TXNIP/NLRP3 pathway in C57 BL/6 mice, International Immunopharmacology, 161, 10.1016/j.intimp.2025.115073, 2025.

Li, X., Li, Y., Lawler, M. J., Hao, J., Smith, J. N., and Jiang, J.: Composition of Ultrafine Particles in Urban Beijing: Measurement Using a Thermal Desorption Chemical Ionization Mass Spectrometer, Environ Sci Technol, 55, 2859-2868, 10.1021/acs.est.0c06053, 2021.

Li, Y., Zhu, T., Zhao, J., and Xu, B.: Interactive Enhancements of Ascorbic Acid and Iron in Hydroxyl Radical Generation in Quinone Redox Cycling, Environmental Science & Technology, 46, 10302-10309, 10.1021/es301834r, 2012.

Liu, F., Yang, X., Xu, W., Verma, V., Wang, Z., Chen, C., He, Y., Yang, L., Yang, Y., Sun, Y., and He, C.: Resolving Organic Aerosol Components Contributing to the Oxidative Potential of PM2.5 in the North China Plain, Journal of Geophysical Research: Atmospheres, 129, 10.1029/2024jd040840, 2024a.

Liu, H., Xu, M., Yang, Y., Cheng, K., Liu, Y., Fan, Y., Yao, D., Tian, D., Li, L., Zhao, X., Zhang, R., and Xu, Y.: The oxidative potential of fine ambient particulate matter in Xinxiang, North China: Pollution characteristics, source identification and regional transport, Environmental Pollution, 360, 10.1016/j.envpol.2024.124615, 2024b.

Liu, W., Xu, Y., Liu, W., Liu, Q., Yu, S., Liu, Y., Wang, X., and Tao, S.: Oxidative potential of ambient PM2.5 in the coastal cities of the Bohai Sea, northern China: Seasonal variation and source apportionment, Environmental Pollution, 236, 514-528, 10.1016/j.envpol.2018.01.116, 2018.

Lopez-Hilfiker, F. D., Iyer, S., Mohr, C., Lee, B. H., D'Ambro, E. L., Kurtén, T., and Thornton, J. A.: Constraining the sensitivity of iodide adduct chemical ionization mass spectrometry to multifunctional organic molecules using the collision limit and thermodynamic stability of iodide ion adducts, Atmospheric Measurement Techniques, 9, 1505-1512, 10.5194/amt-9-1505-2016, 2016.

Lopez-Hilfiker, F. D., Mohr, C., Ehn, M., Rubach, F., Kleist, E., Wildt, J., Mentel, T. F., Lutz, A., Hallquist, M., Worsnop, D., and Thornton, J. A.: A novel method for online analysis of gas and particle composition: description and evaluation of a Filter Inlet for Gases and AEROsols (FIGAERO), Atmospheric Measurement Techniques, 7, 983-1001, 10.5194/amt-7-983-2014, 2014.

Ma, Y., Cheng, Y., Qiu, X., Cao, G., Fang, Y., Wang, J., Zhu, T., Yu, J., and Hu, D.: Sources and oxidative potential of water-soluble humic-like substances (HULIS_{WS}) in fine particulate matter (PM_{2.5}) in Beijing, Atmospheric Chemistry and Physics, 18, 5607-5617, 10.5194/acp-18-5607-2018, 2018.

Mazzoleni, L. R., Zielinska, B., and Moosmüller, H.: Emissions of Levoglucosan, Methoxy Phenols, and Organic Acids from Prescribed Burns, Laboratory Combustion of Wildland Fuels, and Residential Wood Combustion, Environmental Science & Technology, 41, 2115-2122, 10.1021/es061702c, 2007.

McWhinney, R. D., Badali, K., Liggio, J., Li, S.-M., and Abbatt, J. P. D.: Filterable Redox Cycling Activity: A Comparison between Diesel Exhaust Particles and Secondary Organic Aerosol Constituents, Environmental Science & Technology, 47, 3362-3369, 10.1021/es304676x, 2013.

https://doi.org/10.5194/egusphere-2026-4106
Preprint. Discussion started: 14 July 2026

Mohr, C., Lopez-Hilfiker, F. D., Zotter, P., Prevot, A. S., Xu, L., Ng, N. L., Herndon, S. C., Williams, L. R., Franklin, J. P., Zahniser, M. S., Worsnop, D. R., Knighton, W. B., Aiken, A. C., Gorkowski, K. J., Dubey, M. K., Allan, J. D., and Thornton, J. A.: Contribution of nitrated phenols to wood burning brown carbon light absorption in Detling, United Kingdom during winter time, Environ Sci Technol, 47, 6316-6324, 10.1021/es400683v, 2013.

Peng, L., Zhang, Q., Yao, Z., Mauzerall, D. L., Kang, S., Du, Z., Zheng, Y., Xue, T., and He, K.: Underreported coal in statistics: A survey-based solid fuel consumption and emission inventory for the rural residential sector in China, Applied Energy, 235, 1169-1182, 10.1016/j.apenergy.2018.11.043, 2019.

Pye, H. O. T., Ward-Caviness, C. K., Murphy, B. N., Appel, K. W., and Seltzer, K. M.: Secondary organic aerosol association with cardiorespiratory disease mortality in the United States, Nature Communications, 12, 7215, 10.1038/s41467-021-27484-1, 2021.

Ren, S., Yao, L., Wang, Y., Yang, G., Liu, Y., Li, Y., Lu, Y., Wang, L., and Wang, L.: Volatility parameterization of ambient organic aerosols at a rural site of the North China Plain, Atmospheric Chemistry and Physics, 22, 9283-9297, 10.5194/acp-22-9283-2022, 2022.

Shang, Y., Chen, C., Li, Y., Zhao, J., and Zhu, T.: Hydroxyl Radical Generation Mechanism During the Redox Cycling Process of 1,4-Naphthoquinone, Environmental Science & Technology, 46, 2935-2942, 10.1021/es203032v, 2012.

Shen, J., Taghvaee, S., La, C., Oroumiyeh, F., Liu, J., Jerrett, M., Weichenthal, S., Del Rosario, I., Shafer, M. M., Ritz, B., Zhu, Y., and Paulson, S. E.: Aerosol Oxidative Potential in the Greater Los Angeles Area: Source Apportionment and Associations with Socioeconomic Position, Environmental Science & Technology, 56, 17795-17804, 10.1021/acs.est.2c02788, 2022.

Song, S., Ma, T., Zhang, Y., Shen, L., Liu, P., Li, K., Zhai, S., Zheng, H., Gao, M., Moch, J. M., Duan, F., He, K., and McElroy, M. B.: Global modeling of heterogeneous hydroxymethanesulfonate chemistry, Atmospheric Chemistry and Physics, 21, 457-481, 10.5194/acp-21-457-2021, 2021.

Stark, H., Yatavelli, R. L. N., Thompson, S. L., Kang, H., Krechmer, J. E., Kimmel, J. R., Palm, B. B., Hu, W., Hayes, P. L., Day, D. A., Campuzano-Jost, P., Canagaratna, M. R., Jayne, J. T., Worsnop, D. R., and Jimenez, J. L.: Impact of Thermal Decomposition on Thermal Desorption Instruments: Advantage of Thermogram Analysis for Quantifying Volatility Distributions of Organic Species, Environ Sci Technol, 51, 8491-8500, 10.1021/acs.est.7b00160, 2017.

Tuet, W. Y., Chen, Y., Xu, L., Fok, S., Gao, D., Weber, R. J., and Ng, N. L.: Chemical oxidative potential of secondary organic aerosol (SOA) generated from the photooxidation of biogenic and anthropogenic volatile organic compounds, Atmospheric Chemistry and Physics, 17, 839-853, 10.5194/acp-17-839-2017, 2017.

Wang, M., Chen, D., Xiao, M., Ye, Q., Stolzenburg, D., Hofbauer, V., Ye, P., Vogel, A. L., Mauldin, R. L., 3rd, Amorim, A., Baccarini, A., Baumgartner, B., Brilke, S., Dada, L., Dias, A., Duplissy, J., Finkenzeller, H., Garmash, O., He, X. C., Hoyle, C. R., Kim, C., Kvashnin, A., Lehtipalo, K., Fischer, L., Molteni, U., Petaja, T., Pospisilova, V., Quelever, L. L. J., Rissanen, M., Simon, M., Tauber, C., Tome, A., Wagner, A. C., Weitz, L., Volkamer, R., Winkler, P. M., Kirkby, J., Worsnop, D. R., Kulmala, M., Baltensperger, U., Dommen, J., El-Haddad, I., and Donahue, N. M.: Photo-oxidation of Aromatic Hydrocarbons Produces Low-Volatility Organic Compounds, Environ Sci Technol, 54, 7911-7921, 10.1021/acs.est.0c02100, 2020a.

Wang, T., Zhao, J., Liu, Y., Peng, J., Wu, L., and Mao, H.: PM2.5 - Bound Polycyclic Aromatic Hydrocarbons (PAHs), Nitrated PAHs (NPAHs) and Oxygenated PAHs (OPAHs) in Typical Traffic - Related Receptor Environments, Journal of Geophysical Research: Atmospheres, 127, 10.1029/2021jd035951, 2022.

Wang, Y., Wang, M., Li, S., Sun, H., Mu, Z., Zhang, L., Li, Y., and Chen, Q.: Study on the oxidation potential of the water-soluble components of ambient PM2.5 over Xi'an, China: Pollution levels, source apportionment and transport pathways, Environment International, 136, 10.1016/j.envint.2020.105515, 2020b.

https://doi.org/10.5194/egusphere-2026-4106
Preprint. Discussion started: 14 July 2026

Wang, Y., Wang, J., Li, Z., Jin, X., Sun, Y., Cribb, M., Ren, R., Lv, M., Wang, Q., Gao, Y., Hu, R., Shang, Y., and Gong, W.: Contrasting aerosol growth potential in the northern and central-southern regions of the North China Plain: Implications for combating regional pollution, Atmospheric Environment, 267, 10.1016/j.atmosenv.2021.118723, 2021.
Wei, J., Fang, T., and Shiraiwa, M.: Effects of Acidity on Reactive Oxygen Species Formation from Secondary Organic Aerosols, ACS Environmental Au, 2, 336-345, 10.1021/acsenvironau.2c00018, 2022.
Yan, C., Zheng, M., Bosch, C., Andersson, A., Desyaterik, Y., Sullivan, A. P., Collett, J. L., Zhao, B., Wang, S., He, K., and Gustafsson, O.: Important fossil source contribution to brown carbon in Beijing during winter, Sci Rep, 7, 43182, 10.1038/srep43182, 2017.
Yu, Q., Chen, J., Qin, W., Ahmad, M., Zhang, Y., Sun, Y., Xin, K., and Ai, J.: Oxidative potential associated with water-soluble components of PM2.5 in Beijing: The important role of anthropogenic organic aerosols, Journal of Hazardous Materials, 433, 10.1016/j.jhazmat.2022.128839, 2022.
Zha, Q., Aliaga, D., Krejci, R., Sinclair, V., Wu, C., Ciarelli, G., Scholz, W., Heikkinen, L., Partoll, E., Gramlich, Y., Huang, W., Leiminger, M., Enroth, J., Peräkylä, O., Cai, R., Chen, X., Koenig, A. M., Velarde, F., Moreno, I., Petäjä, T., Artaxo, P., Laj, P., Hansel, A., Carbone, S., Kulmala, M., Andrade, M., Worsnop, D., Mohr, C., and Bianchi, F.: Oxidized organic molecules in the tropical free troposphere over Amazonia, National Science Review, 10.1093/nsr/nwad138, 2023.
Zhang, J., Peng, J., Song, A., Lv, Z., Tong, H., Du, Z., Guo, J., Wu, L., Wang, T., Hallquist, M., and Mao, H.: Marked impacts of transient conditions on potential secondary organic aerosol production during rapid oxidation of gasoline exhausts, npj Climate and Atmospheric Science, 6, 10.1038/s41612-023-00385-4, 2023.
Zhang, Q., Ma, H., Li, J., liu, F., Jiang, H., Huang, J., Jiang, B., You, J., Dong, G., Li, Q., Ma, W., Yu, Z., and Zhang, G.: Unveiling Condensed Aromatic Amines as Noteworthy Genotoxic Components in PM2.5 Dissolved Organic Matter, Environmental Science & Technology, 59, 21015-21027, 10.1021/acs.est.5c07412, 2025.
Zhang, T., Luan, M., Zhou, Q., Liu, J., Wei, Y., Wei, J., Wang, Q., Zhang, L., Shen, X. e., Sun, Z., Tian, C., and Zheng, M.: Changes in chemical composition of dust aerosols during transport: Elevated risks for human health but enhanced nutrient supply for marine ecosystem, Atmospheric Environment, 382, 10.1016/j.atmosenv.2026.122168, 2026.
Zhang, X., Staimer, N., Tjoa, T., Gillen, D. L., Schauer, J. J., Shafer, M. M., Hasheminassab, S., Pakbin, P., Longhurst, J., Sioutas, C., and Delfino, R. J.: Associations between microvascular function and short-term exposure to traffic-related air pollution and particulate matter oxidative potential, Environmental Health, 15, 10.1186/s12940-016-0157-5, 2016.
Zheng, F., Li, J., Hua, C., Liu, T., Xie, J., Feng, Z., Zhang, Y., Yan, C., Xia, M., Yuan, Q., Bianchi, F., Petäjä, T., Kerminen, V.-M., Kulmala, M., Daellenbach, K. R., Cai, J., and Liu, Y.: Comparative analysis of multiple health risks from different air pollution events, Journal of Environmental Sciences, https://doi.org/10.1016/j.jes.2026.02.033, 2026.
Zheng, Y., Chen, Q., Cheng, X., Mohr, C., Cai, J., Huang, W., Shrivastava, M., Ye, P., Fu, P., Shi, X., Ge, Y., Liao, K., Miao, R., Qiu, X., Koenig, T. K., and Chen, S.: Precursors and Pathways Leading to Enhanced Secondary Organic Aerosol Formation during Severe Haze Episodes, Environmental Science & Technology, 55, 15680-15693, 10.1021/acs.est.1c04255, 2021.
Zhou, J., Elser, M., Huang, R.-J., Krapf, M., Fröhlich, R., Bhattu, D., Stefenelli, G., Zotter, P., Bruns, E. A., Pieber, S. M., Ni, H., Wang, Q., Wang, Y., Zhou, Y., Chen, C., Xiao, M., Slowik, J. G., Brown, S., Cassagnes, L.-E., Daellenbach, K. R., Nussbaumer, T., Geiser, M., Prévôt, A. S. H., El-Haddad, I., Cao, J., Baltensperger, U., and Dommen, J.: Predominance of secondary organic aerosol to particle-bound reactive oxygen species activity in fine ambient aerosol, Atmospheric Chemistry and Physics, 19, 14703-14720, 10.5194/acp-19-14703-2019, 2019.